SAPIENZA

UNIVERSITA' DI ROMA

DOTTORATO DI RICERCA IN MEDICINA SPERIMENTALE
XXIV CICLO

Role of the mesothelial microenvironment in the peritoneal dissemination of gastric and colorectal cancers

DOTTORANDO

Danilo Ranieri

DOCENTE GUIDA

Salvatore Raffa

COORDINATORE DEL DOTTORATO
Prof.ssa Maria Rosaria Torrisi

ANNO ACCADEMICO 2010-2011

1. Introduction

The peritoneal spreading of gastric and colorectal cancers represents a frequent event occurring after curative resection (Sadeghi et al. 2000, Jaine et al. 2002). Critical for the peritoneal recurrence is the adhesion of the free disseminated cancer cells to the mesothelial layer and many different molecular mechanisms directly involved in this process have been identified. For peritoneal carcinomatosis, cancer cells must be able to survive in the peritoneal cavity, once detached from the primary tumor, and must display a proliferative and invasive behaviour, once adhered to the mesothelium.

The first step in the development of peritoneal carcinomatosis is the detachment of tumour cells from the primary cancer, a spontaneous shedding of loose cell like a result of rapid tumor cell proliferation (Hayashi et al., 2007). Once detached, cells are transported through the peritoneal cavity along predictable routes. Both of these carcinomas can spread to other organs with haematogenous metastasis, regional lymph node metastasis and peritoneal dissemination (Pantel et al., 2008). The interaction between the forces of gravity, diaphragmatic excursion, mesenteric reflections, and peritoneal recesses results in a flow directed towards the pelvis and from the pelvis, along the right paracolic gutter, towards the subdiaphragmatic space. Moreover, cancer cells have inherent motility provided by lamellipodia and filipodia; cell structures that generate force by polymerisation of actin microfilaments, a process stimulated by the binding of growth factors to the

membrane (Celeen et al., 2009). Loose cancer cells can adhere to mesothelial cells, the extracellular matrix, or to specialised structures, such as the omentum and the diaphragmatic peritoneum.

1.1 Role of mesothelial microenvironment in the peritoneal dissemination

Adhesion of cancer cells to the mesothelial layer is mediated by several adhesion molecules, many of which are also expressed by endothelial cells (Table 1).

Many studies have been addressed to the analysis of the expression and activation of molecular pathways responsible for the sequential biological changes of the different types of cancer cells (Harada et al. 2001, Kajiyama et al. 2008, Saito et al. 2010).

Numerous Authors have demonstrated that adhesion of tumour cells to the hyaluronan pericellular coat of mesothelial cells is an important step in the peritoneal spread of ovarian and colorectal cancer (Casey et al., 2003).

A wide variety of malignancies of epithelial and mesenchymal origin express high levels of the hyaluronan receptor CD44. Blocking interaction of CD44 with hyaluronan using antisense CD44 cDNA monoclonal antibodies that block the hyaluronan binding site of CD44, intact hyaluronan and hyaluronan oligomers, reduced cell adhesion and inhibited cell migration. However, because blocking CD44 did not totally inhibit mesothelial binding in all studies, it is likely that other surface molecules are involved (Cannistrà et al., 1993; Casey et al., 2003).

ECM components	Urokinase plasminogen activator (uPA) and its receptor (uPAR), Vitronectin	Madsen et al, *J Cell Biol*, 2007 Heyman et al, *Tumor Biol*, 2008
Integrins	α2, α3, α5 and β1	Saito et al, *Clin Exp Metastasis*, 2010 Felding, *Clin Exp Metastasis*, 2003 Takatsuki et al, Cancer Research, 2004
ECM components	Laminin-5	Saito et al, *Clin Exp Metastasis*, 2010 Nakashio et al, *Int. J. Cancer*, 1997
Metalloproteinases	MMP-9	Saito et al, Clin Exp Metastasis,2010 Kim et al, Anticancer Res, 2004
Antigens	CEA (Carcinoembrionic antigen)	Tomita et al, *Immunology*, 1974
Growth Factor	TGF-β1	Nakashio et al, *Int. J. Cancer*, 1997
Cell adhesion molecule (CAM)	CD44H, CD44E, CD133, ICAM-1, VCAM-1, PECAM	Nakashio et al, *Int. J. Cancer*, 1997 Orian, *Eur J Cancer*, 2010 Jayne et al, *Clin Exp Metastasis*, 1999 Haraguchi et al, *Ann Surg Oncol*, 2008 Takatsuki et al, *Cancer Research*, 2004
ECM components	Hyaluronic acid	Nakashio et al, *Int. J. Cancer*, 1997
ECM components	Collagen 1and 4	Nakashio et al, *Int. J. Cancer*, 1997 Jayne et al, *Clin Exp Metastasis*, 1999
ECM components	Fibronectin	Nakashio et al, *Int. J. Cancer*, 1997
Cytokines	TNF-α, IL-1β, IL-6, IL-8	Jayne et al, *Clin Exp Metastasis*, 1999 Mochizuchi et al, *Clin Exp Metastasis*, 2004 Van Grevenstein et al, *Dig Dis Sci*, 2007

Table 1. Molecules involved in the adhesion of cancer cells to mesothelial monolayer.

The role of integrins in the interaction of tumour cells with mesothelial cells has also been explored. Lessan *et al.* demonstrated that is possible reduce adhesion of an ovarian carcinoma cell line to mesothelial cells by using a monoclonal antibody against the β1 integrin subunit, which is common to many integrin molecules and can bind a variety of ECM proteins (Casey et al., 2003)

Migration of ovarian carcinoma cell lines towards fibronectin, type IV collagen and laminin can be blocked by antibodies against α5β1, α2β1 and α6β1, respectively. Equally, antibodies against CD44 reduced cell adhesion and migration, suggesting that tumour migration is regulated by both integrin-dependent and independent mechanisms (Jones et al., 1995; Casey et al., 2003)

Although mesothelial cells appear to mainly promote tumour dissemination and growth, intact hyaluronan inhibits the adhesion of tumour cells to mesothelium. Similarly, conditioned medium from a confluent mesothelial cell culture containing high amounts of hyaluronan prevented tumour cell attachment to mesothelial cells, but hyaluronidase treatment increased tumour cell adhesion. Free hyaluronan in the conditioned medium would have bound to the CD44 molecules on the tumour cells and blocked their interaction with the hyaluronan present on the surface of the mesothelial cells.

Removal of free hyaluronan may explain why tumour cells adhere to mesothelial cells in other studies. Therefore, under normal physiological conditions, secretion of hyaluronan by mesothelial cells into the serosal fluid may protect the serosal surface from tumour implantation.

A limited number of reports have focused on the contribution of the mesothelial layer in the adhesion and peritoneal spreading of the cancer (Casey et al. 2003, Takatsuki et al. 2004, Alkhamesi et al. 2005). However, as discussed, mesothelial cells synthesize a host of growth factors in response to inflammatory stimuli and, therefore, may play a role in stimulating tumour growth. Several experimental studies have demonstrated that, following surgical trauma, tumour growth is also enhanced at sites distal to the injury (Bouvy et al., 1997; van den Tol et al., 1998). In addition, increased tumour growth was observed in animals exposed to surgical wound fluid or a combination of the growth factors TGF-β and bFGF, suggesting that mediators produced after surgical trauma enhance local and distant tumour growth (Hofer et al., 1998). It is likely that these mediators induce upregulation of cell adhesion molecules on mesothelial cells, promoting tumour cell attachment. Once the tumour cells adhere to mesothelial cells, they can migrate through the mesothelium, invade local organs and move to distant sites. Interleukin-1β, TNF-α and IFN-γ upregulate adhesion molecule expression on mesothelial cells and IL-1β and EGF increase tumour cell adhesion to cultured mesothelial cells. Adhesive interactions were also reported between the mesothelial hyaluronan coat and the transmembrane glycoprotein CD44, a molecule expressed by many cancer types.

Interactions have been noted between chemokine receptors present on the cancer cells and mesothelial targets. Examples include binding of CXCR4 to stromal cell-derived factor 1 (SDF-1) and binding of MUC16 to mesothelin. In areas of absent or contracted mesothelial cells, interaction between cancer cells and the underlying

extracellular matrix components—laminin and fibronectin—seems mainly mediated by the ®1 integrin subunit.

Resting mesothelial cells have been shown to express vascular, intercellular, and platelet endothelial cell adhesion molecules (VCAM-1, ICAM-1, and PECAM-1). Experimental evidence showed that, in vitro, adhesion is mediated by the interaction of mesothelial ICAM-1 and CD43 of tumor cells (sialophorin) rather than ®2 integrin, the most ubiquitous ligand of ICAM-1 (Celeen et al. 2009).

For the detailed analysis of the molecular mechanisms affecting the adhesive stage, different in vitro or ex-vivo models have been developed (Jayne et al. 1999, Cabourne et al. 2010) and primary cultures of mesothelial cells have been obtained to test the adhesion of cancer cells in presence of promoting or interfering agents (Casey et al. 2003, Heyman et al. 2008). Most of these models utilize either established cell lines or human primary cultures of mesothelial cells isolated from omental fragments (Yung et al. 2006, Sikkink et al. 2009). However, it has been proposed that also the peritoneal lavages are a good and more practical source of mesothelial cells to be propagated in vitro (Ivarsson et al. 1998), although their use in co-culture models has not been explored.

Adhesion molecules play a major role in the step involving the attachment of the free cancer cells to the peritoneal surface (Celeen et al. 2009) and cytokines, such as interleukin 1β (IL1β and tumor necrosis factor α (TNFα) released in the inflammatory microenvironment, are known to promote their expression (Van Grevenstein et al. 2007, Ziprin et al. 2003). Among the adhesion molecules which

play a key role in the spreading of the neoplastic cells to the mesothelial monolayer, several studies pointed to the specific function of the intercellular adhesion molecule 1 (ICAM1) present on the mesothelial cells in promoting the process (Alkhamesi et al. 2005, Ziprin et al. 2003); in addition, it has been shown that the up-modulation of its expression, as a result of oxidative stress and senescence of the peritoneal cells, promotes the adhesion of neoplastic cells from ovarian, gastric and colon cancers (Ksiazek et al. 2008, 2009, 2010), demonstrating the general and crucial role of ICAM1 in the spreading.

1.2 Role of tumoral counterpart in the peritoneal dissemination: the free peritoneal tumor cells (FPTCs)

The role played by the tumoral counterpart in gastric cancer and colorectal cancer represent the other side of the carcinomatosis disease.

The peritoneal dissemination is more frequent in gastric cancer than in colorectal cancer and is due to the detachment of epithelial cells from primary solid tumor (Khair et al. 2007, Pantel et al. 2008).

Peritoneal dissemination by primary gastric and colorectal tumor is an important step in metastatic cascade and free cancer cells have been detected by cytological examination of peritoneal washes (Hayes et al. 1999).

The success of surgical treatment in patients with gastric and colorectal cancer is often limited. This is because of local recurrence or the development of distant metastases or peritoneal carcinomatosis by cells that have already been seeded at

the time of operation but cannot be detected using conventional diagnostic tools. The elimination of these micrometastatic cells is the aim of various adjuvant therapies (Hagiwara et al. 1992, Moertel et al. 1990); therefore, it is very important to examine the presence or absence of free cancer cells in the peritoneal cavity at the time of surgery (Bando et al. 1999, Kodera et al. 1999). However, it remains unclear if single tumor cells are of prognostic significance and have the ability to form metastatic disease.

Peritoneal lavage cytology is the gold standard for assessing the presence of peritoneal dissemination of gastric and colorectal cancer, but its sensitivity is relatively low, ranging 14-21% in gastric cancer involving the serosa (Juhl et al. 1994, Wu et al. 1997, Benevolo et al. 1998). Recently, several new methods for detecting micrometastasis, including immunochemical and biological methods have been developed (Nekarda et al. 1999, Kodera et al. 2002, Sakakura et al. 2004). Among other techniques, immunocytochemistry and real time quantitative reverse-transcriptase polymerase chain reaction (qRT-PCR) techniques have been used to improve the sensitivity of this method (Benevolo et al. 1998). Molecular characterization by real-time qRT-PCR of cellular tumour markers could contribute to understand the role of tumour dormant cells and have a good prognostic value in patients with colorectal and gastric cancer after curative surgery (Baba et al. 1989). Recently, molecular diagnosis with real-time qRT-PCR was performed to detect free cancer cells from peritoneal washing in patients with advanced gastric cancer (Kodera et al. 1998).

The carcinoembryonic antigen (CEA), cytokeratin-20 (CK20) and cytokeratin-19 (CK19) are the most common target for real-time qRT-PCR amplification in peritoneal washes from gastric cancer patients (Katsuragi et al. 2007). In particular, CEA and CK20 evaluated with multivariate analysis represent independent prognostic markers (Oyama et al. 2004). However, it has been also argued that the detection of these markers by RT-PCR-based methods is of limited value because both CEA and CK20 can be expressed and released by hematopoietic cells in the inflammatory context (Kowalewska et al. 2008).

2. High adhesion of cancer cells to mesothelial monolayer derived from peritoneal wash.

2.1 Aims

In the attempt to better define the mesothelial contribution to the adhesion of cancer cells and, in particular, the possible role of the mesothelial activation in a cancerous environment mimicking in vitro as much as possible the in vivo conditions, we used here a direct adhesion test performed on human primary cultures of mesothelial cells (HPMCs) derived from the peritoneal washes of patients with gastric and colorectal tumors or of patients with benign diseases, in order to mimic in vitro as much as possible the in vivo conditions. With the aim to minimize the possible variations attributable to the tumor counterpart, we matched different isolated HPMCs, grown also at different levels of senescence, with two well known cancer cell lines. Our results show that the adhesive behaviour of the cancer cells is not affected by the origin of the HPMCs from patients with different tumors. However, our observations confirm the role of the peritoneal senescence, through the enhanced production of reactive oxygen species and of ICAM1 expression, in promoting the tumor cell adhesion (Ksiazek et al. 2008, 2009, 2010) and suggest that the use of the peritoneal washes as a source to isolate and propagate HPMCs can be easily applied to evaluate in vitro the state of the mesothelium in cancer patients.

2.2 Materials and methods

2.2.1 Cell lines

The human mesothelial MeT-5A cell line was cultured in Dulbecco's modified eagle's/F12 medium (DMEM/F12) supplemented with 10% fetal bovine serum (FBS) plus antibiotics and hydrocortisone (0,1 μg/ml), insulin (2,5 μg/ml), transferrin (2,5 μg/ml) and selenium (2,5 ng/ml) (Sigma Chemicals Co., St Louis, MD, USA). The human colorectal adenocarcinoma Caco2 cell line was cultured in Dulbecco's Modified Eagle's Medium (DMEM) supplemented with 10% FBS plus antibiotics (Sigma). The human gastric adenocarcinoma AGS cell line was cultured in Ham's F12 medium (Sigma) supplemented with 10% FBS plus antibiotics (Sigma).

2.2.2 Primary cultures

Primary cultures of Human Peritoneal Mesothelial Cells (HPMCs) were obtained from intraoperatively peritoneal lavages of patients affected by colorectal cancer (n. 48), gastric cancer (n. 27) and non-cancerous diseases (n. 6), who underwent surgery between December 2008 and December 2009 at the A Unit of Surgery of Sant'Andrea Hospital.

All patients were extensively informed and gave written consent for the investigation. To avoid possible activation of the peritoneal cells by the surgical process, the peritoneal lavages were obtained at the starting steps of the surgery.

From each patient, 40 mL of peritoneal wash were collected in EDTA (50 μM).

The peritoneal washes were centrifuged at 1100 rpm for 5 minutes at RT and pelletted. Samples were resuspended for magnetic labeling in 80 μL of MACS® separation buffer (Miltenyi Biotec, Bergisch Gladbach, Germany). To remove epithelial cell component from the peritoneal wash and consequently to enrich the mesothelial portion, immunomagnetic depletion using anti-CD326/EpCAM microbeads (Miltenyi Biotec, Bergisch Gladbach, Germany) was performed according to the manufacturer's instructions.

Briefly, MS separation columns (MACS®, Miltenyi Biotec) had been equilibrated with 0,5 mL of MACS® separation buffer and the microbeads labeled cells were subjected to magnetic field trough the column passage. The CD326 negative cells were washed off from the column, and were plated in DMEM/F12 as above.

For the adhesion experiments, we have used three representative HPMCs primary cultures: #Ctrl2 (from a patient with non-cancerous disease), #062 (from a patient affected by colon cancer) and #219 (from a patient affected by gastric cancer). The donor clinico-pathological characteristics are described in Table 1.

2.2.3 Co-cultures

For co-culture experiments, MeT-5A or HPMCs were grown to confluence and after 24h Caco2 or AGS cells were seeded on the monolayer.

2.2.4 Immunofluorescence

For HPMCs characterization cells were grown on coverslips and fixed with 4% paraformaldehyde followed by treatment with 0,1 M glycine for 20 minutes at 25°C and with 0,1% Triton X100 for an additional 5 minutes at 25°C to allow permeabilization. Cells were then incubated for 1 hour at 25°C with the following primary antibodies: anti-cytokeratins (recognizing CK8 and CK19 among other CKs) (1:100 in PBS; clone MNF116; Dako, Glostrup, Denmark) monoclonal antibody; anti-vimentin (1:100 in PBS; clone V9; Dako) monoclonal antibody; anti-calretinin (1:100 in PBS; clone DAK Calret 1; Thermo Fisher Scientific Inc., Fremont, CA, USA) monoclonal antibody; anti-CEA (1:100 in PBS; Zymed, Invitrogen, Carlsbad, CA, USA) polyclonal antibodies; anti-EpCAM (1:10 in PBS; Miltenyi Biotec GmbH, Bergisch Gladbach, Germany) monoclonal antibody directly conjugated with PE; anti-ICAM1 (1:10 in PBS; Stemcell Technologies, Vancouver, BC, Canada) monoclonal antibody directly conjugated with FITC.

The unconjugated primary antibodies were visualized, after appropriate washing with PBS, using goat anti-mouse FITC (1:50 in PBS; Cappel Research Products, Durham, NC), goat anti-mouse Texas Red (1:200 in PBS; Jackson Immunoresearch

Laboratories, West Grove, PA, USA), goat anti-rabbit FITC (1:400 in PBS; Cappel Research). To identify cycling cells, immunostaining was performed with anti-Ki67 rabbit polyclonal antibodies (1:50 in PBS; Zymed Laboratories, San Francisco, CA). Nuclei were stained with 4',6-diamidino-2-phenylindole (DAPI) (1:10.000 in PBS; Sigma). Coverslips were finally mounted with 90% glycerol in PBS for observation. Fluorescence signals were visualized with the ApoTome System (Zeiss, Oberkochen, Germany) connected with an Axiovert 200 inverted microscope (Zeiss) and image analysis was performed by the Axiovision software (Zeiss) and KS300 Image processing system (Zeiss).

Percentage of EpCAM/Ki67-positive cells in co-cultures of MeT-5A and AGS or Caco2 cells was analyzed counting a total of 500 cells randomly observed in 5 microscopic fields for each different time points (1h, 24h, 48h) during the time course of the experiment.

Percentage of ICAM-1-positive cells in HPMCs was analyzed counting for each primary culture a total of 300 cells, randomly observed in 10 microscopic fields from three different experiments. Quantitative analysis of the ICAM-1 fluorescence intensity was performed by the analysis of 100 cells for each sample in five different fields, randomly taken from three different experiments.

All results were expressed as mean values ± SE. Significance was calculated using Kruskal-Wallis test or Student's t test; p values < 0.05 were considered statistically significant.

2.2.5 Adhesion assay

Subconfluent Caco2 or AGS cells were trypsinized and resuspended in DMEM serum free and labeled with 5 ⌈l/ml of Vybrant®DiI solution (Invitrogen, Carlsbad, CA, USA) by incubation for 30 minutes at 37°C. The DiI-labeled cells were washed three times and resuspended in DMEM/F12 as above. The labeled-cells were directly plated on the mesothelial monolayer ($25X10^3/cm^2$ of monolayer) and incubated for 1, 24, 48 hours. In the adhesion assays with the anti-ICAM1 blocking antibody (Stemcell Technologies), the incubation was performed in the presence of different dilutions (1:10, 1:5, 1:2) of the antibody (specificare I tempi). Non-adherent cells were removed by abundant washes with serum free medium, and adherent cells and HPMCs monolayers were fixed with 4% paraformaldehyde, followed by treatment with 0.1M glycine for 20 minutes at 25°C and with 0.1% Triton X-100 for additional 5 minutes at 25°C to allow permeabilization. Nuclei were stained with DAPI. Nuclei were stained with DAPI (42,6-diamidino-2-phenylindol) (1:10.000 in PBS; Sigma).

Quantitative analysis of DiI-positive cells/mm2 was performed by counting the number of positive cells in 10 different optical fields of 2,24 mm^2, randomly taken from three different experiments. Results have been expressed as mean values ± SE. P values were calculated using Kruskal-Wallis test and significance level was defined as $p<0,05$.

2.2.6. Reactive oxygen species detection

For reactive oxygen species (ROS) detection, HPMCs cells were incubated with 2',7'-dichlorofluorescein diacetate (DCFH-DA, Fluka) (5 μM) for 10 min at 37°C, washed extensively with PBS and immediately observed under an Axioskop 2 microscope equipped with Pascal LSM 5 confocal laser scan (Zeiss, Oberkochen, Germany) using an argon laser with a 488 nm excitation band. The emission long pass was a 505 filter: laser intensity, pinhole diameter and photomultiplier settings were kept constant for every experiment. Fluorescence images were analyzed by KS300 (Zeiss). The fluorescence intensity was measured by image analysis evaluating at least 200 cells for each condition in three different microscopic fields. The data presented are expressed as mean values ± SE from three different experiments. Statistical analysis was performed using Student's t test and significance level has been defined as $p<0,05$.

2.3 Results

2.3.1 Optimization of the in vitro test for evaluation of the adhesion of cancer cells to the mesothelial monolayers

One of the first key step in peritoneal metastatic dissemination of gastrointestinal tumours is the adhesion of cancer cells to the mesothelial monolayer (4). To study the biological behaviour of both cancer and mesothelial cells and to evaluate their properties of adhesion, we first selected and adapted to our conditions a co-culture

system and an in vitro test for adhesion (Fig. 1A), previously used for ovarian cancer (12). The human mesothelial cell line MeT-5A was grown at confluence and human gastric adenocarcinoma cells (AGS cell line) or human colon carcinoma cells (Caco2 cell line) were seeded in co-culture at the density of 25.000 cells/cm^2 of mesothelial monolayer.

To identify the different cell types in our co-culture model, we used immunofluorescence (IF) microscopy. After 24 hours from seeding, to recognize the mesothelial cells making up the Met-5A monolayer, we stained the co-cultures with a primary antibody directed against vimentin, a component of the intermediate filaments of the cytoskeleton, followed by a secondary Ab labeled with the FITC fluorocrome (green): the signal was compatible with the structure and localization of vimentin, which appears as perinuclear cytoplasmic bundles of filaments (Fig. 1B). The cancer cells were labeled with ⟨-EpCAM PE antibody, recognizing a human epithelial adhesion molecule and directly conjugated to the fluorochrome PE (red): the corresponding signal was associated with the plasma membrane of the cells adherent to the monolayer (Fig. 1B). The cellular nuclei were stained with DAPI (blue). Both AGS and Caco2 cells appeared either in small clusters or isolated and strictly adherent to the mesothelial cells (Fig. 1B).

For the evaluation of the adhesive properties of the cancer cells, we used phase contrast microscopy, which allowed to verify the mesothelium monolayer and removed any doubt about the possibility of cancer cells adhering to the glass or plastic support. The morphological analysis after 48 hours from seeding showed

A

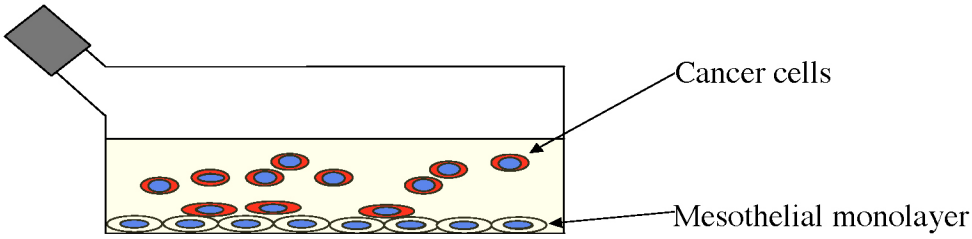

AGS

Caco2

B

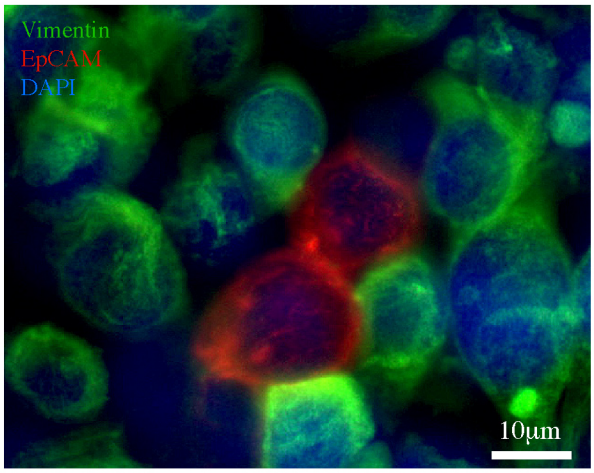

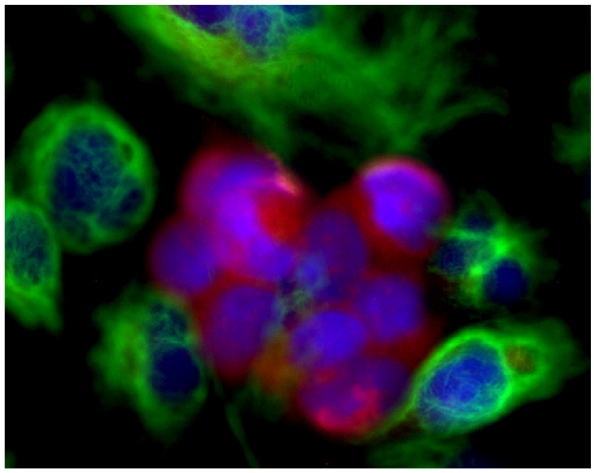

C

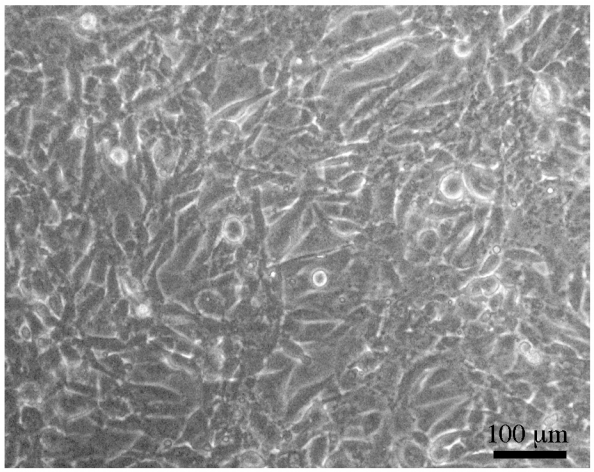

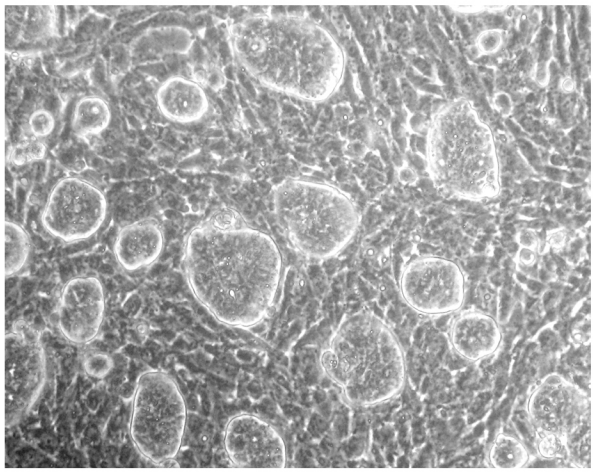

D

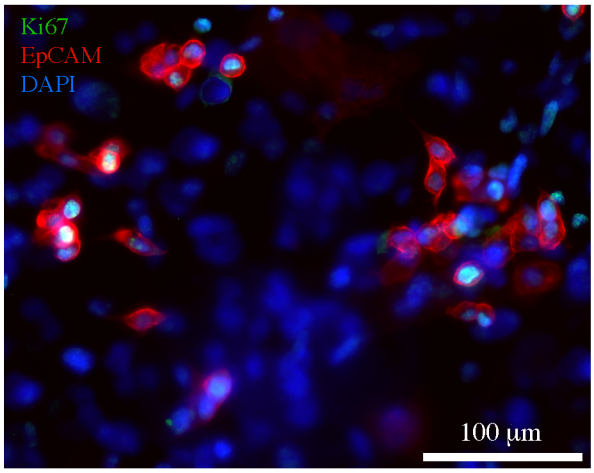

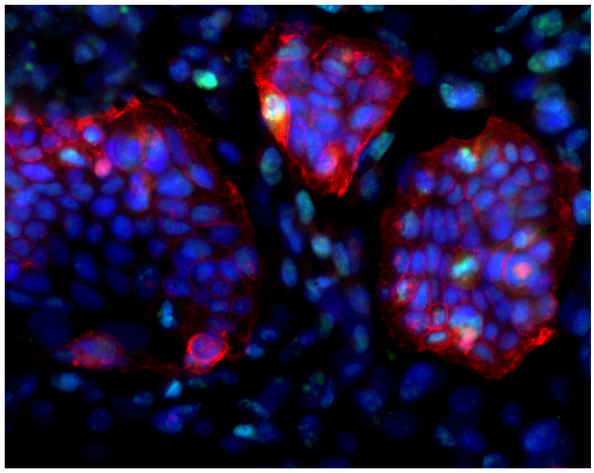

Figure 1. Co-culture in vitro test for the adhesion of cancer cell lines to mesothelial monolayer.

A) Schematic drawing of the co-culture system and the adhesion test used throughout the study: cancer cells are seeded on a mesothelial monolayer to evaluate cell adhesion.

B) MeT-5A mesothelial cell line was grown at confluence and AGS or Caco2 cells were seeded on the mesothelial monolayer in co-culture (25.000 cells/cm2). After 24 hours from seeding, the co-culture was fixed, permeabilized and stained with a primary antibody directed against vimentin, followed by a secondary Ab labeled with the FITC fluorocrome (green) to identify the mesothelial cells. Double immunofluorescence with α-EpCAM PE antibody (red) was performed to recognize the cancer epithelial cells. Cellular nuclei were stained with DAPI (blue). The immunofluorescence analysis reveals the different cell types in our co-culture model. The signal corresponding to vimentin in the cell monolayer is compatible with that of intermediate filaments, as perinuclear cytoplasmic bundles, while the EpCAM staining is associated with the plasma membrane of the cancer cells. Both AGS and Caco2 cells appear either in small clusters or isolated and strictly adherent to the mesothelial cells. Bar: 10 μm

C) Phase contrast microscopy used to verify the integrity of mesothelium monolayer. After 48 hours from seeding, the adherent Caco2 cells display a pattern of growing in compact islands, while the AGS adhering cells show a more flattened shape and an isolated pattern of growth. Bar: 100 μm

D) Proliferation assay performed by immunofluorescence staining with a primary anti-Ki67 antibody, which identifies cycling cells, followed by a secondary FITC-labeled Ab (green). The tumor cells were labeled with the anti-EpCAM PE Ab as above. After 48 hours from seeding, the distribution of the cancer cells positive for the Ki67 nuclear signal reveals a different behavior of tumor growth: differently from the isolated AGS cells, the Ki67+ Caco2 cells are located at the periphery of the islands. Bar: 100 μm

that the adherent Caco2 cells displayed a pattern of growing in compact islands (Fig. 1C). In contrast, the AGS adhered cells were characterized by a more flattened shape and a more isolated pattern of growth (Fig. 1C).

To better understand the biological behaviour observed in phase contrast microscopy and to evaluate the proliferation rate of the adherent cells, we used IF analysis with the Ki67 marker which identifies cycling cells. After 48 hours from seeding, the co-cultures were stained with a primary anti-Ki67 antibody, followed by a secondary FITC-labeled Ab (green).

The tumor cells were labeled with the anti-EpCAM PE Ab as above. While the proliferative rate of the two adhering cell types, evaluated as the percentage of the the cells positive for the Ki67 nuclear signal was comparable (21%±2 and 23%±2 for the Caco2 and AGS cells respectively; Kruskal-Wallis test: p=NS), their distribution revealed a different behaviour of the cancer cells (Fig. 1D). In fact, unlike AGS cells, the Ki67+ Caco2 cells were located at the periphery of the islands, as expected from their spontaneous ability to differentiate in vitro (Visco et al., 2004).

For a quantitative evaluation of the adhesion of the two cancer cell lines to the MeT-5A monolayer, we used the lipophilic cellular tracer DiI to label the cancer cells before the adhesion test (Heyman et al., 2008). Figure 2A shows the results obtained by the contemporary use of DiI and DAPI staining of the co-cultures at different time points (1h, 24h, 48h) from seeding. Images of 10 different optical fields were randomly taken as described in materials and methods. The numbers of DiI+ cancer cells per mm^2 were then calculated and statistically analyzed as described in

A

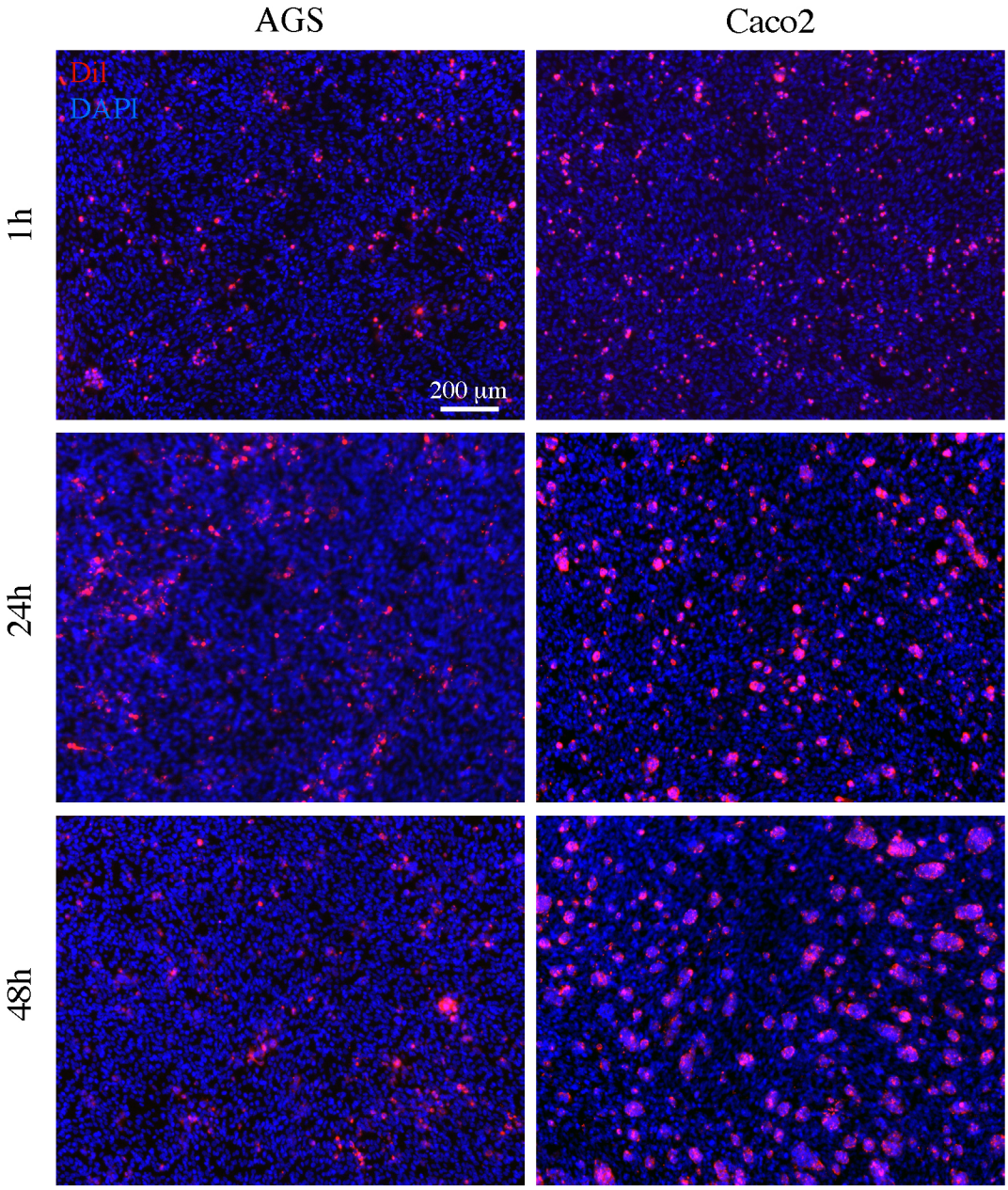
AGS
Caco2
DiI
DAPI
200 µm
1h
24h
48h

B

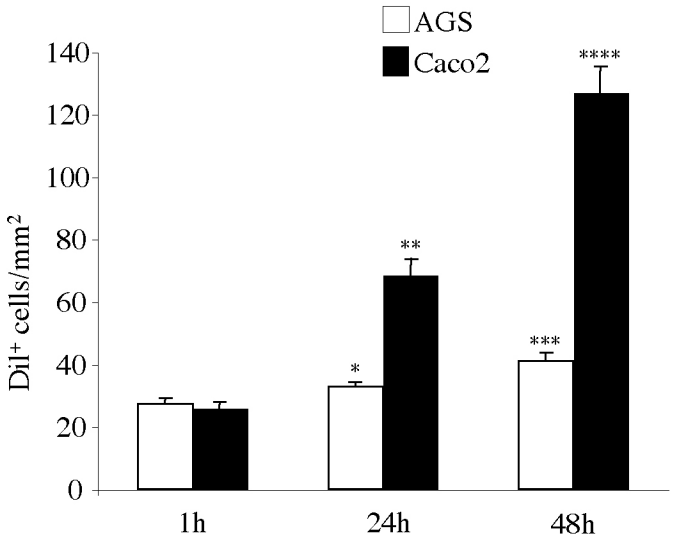
AGS
Caco2
DiI+ cells/mm2
140
120
100
80
60
40
20
0
1h
24h
48h
*
**
***
****

Figure 2. Adhesion test with AGS and Caco2 cells on Met-5A monolayer
A) Met-5A mesothelial monolayer was grown as described above. Caco2 and AGS cells were labeled with the Dil tracer and then seeded on the monolayer as above. After 1, 24 and 48 hours, co-cultures were washed, fixed and permeabilized. Nuclei were stained with DAPI. Bar: 200 μm
B) Quantitative analysis of the number of adherent Dil+ cells/mm2 was performed as described in materials and methods. While after 1 hour of seeding both Caco2 and AGS cells adhere to the monolayer in equal amount, at the 24 and 48 hours time points the number of Caco2 cells is almost doubled compared to that of AGS, which increases only slightly but significantly over the time. Results are expressed as mean values ± IC 95%. Student's t test was performed and significance levels have been defined a $p<0,05$. *$p<0,001$ vs the corresponding 1 hour; **$p<0,001$ vs the corresponding 1 hour and 24 hours.

materials and methods. The results in figure 2B showed that both Caco2 and AGS cells were adhering to the mesothelial monolayer in equal amount at 1 h of co-culture. However, adhesion of Caco2 cells had the tendency to double after 24 and 48 hours, while the AGS cells, although slightly but significantly increasing in number during the timespan, were less numerous than the Caco2 cells at either time points ($p<0,05$). Because the proliferative rate of the two cell types at 48 hours, as described above, did not reveal differences which may account for the higher number of Caco2 cells adhering to the monolayer compared to the AGS cells, the results of the DiI-based test appeared to reflect real differing adhesive properties.

2.3.2 Adhesion of cancer cells to primary human mesothelial monolayer derived from peritoneal washes

To assess the possible role of the mesothelium in the adhesion process of the cancer cells in our co-culture system, we used the above test with primary cultures of mesothelial cells obtained from the peritoneal wash of patients affected by colorectal or gastric cancer and non-carcinoma disease. In fact, the peritoneal lavage represents a practical source of mesothelial cells (Ivarsson et al., 1998), instead of utilizing omentum fragments.

To characterize the human peritoneal mesothelial cells (HPMCs), obtained as described in materials and methods, we used immunofluorescence microscopy (Fig. 3). To recognize the primary mesothelial cells from other types of cells present in the peritoneal wash, such as fibroblasts and epithelial cancer cells, we stained the

cultures with a combination of antibodies directed against known mesothelial markers, such as vimentin, cytokeratins (CK8 and CK19) and calretinin. To be sure that the cells were of mesenchimal origin and not epithelial, we used in parallel the same antibodies on Caco2 cells. The results showed that the HPMCs were positive for both vimentin and cytokeratin staining, which appeared as perinuclear cytoplasmatic bundles of intermediate filaments (Fig. 3, left panels). As expected, Caco2 cells were negatively stained for vimentin and positively labeled for cytokeratins (Fig. 3, right panels). To unequivocally discriminate the HPMCs from fibroblasts possibly present in our cultures, cells were labeled with antibodies against calretinin, an intracellular calcium-binding protein belonging to the troponin-C superfamily expressed in mesothelial cells: the signal was in cytosolic hot-spots (Fig. 3, right panel). Again, the epithelial Caco2 cells were negative (Fig. 3, left panel). In contrast, HPMCs were negative for the epithelial marker EpCAM which was expressed on the plasma membranes of the Caco2 cells (Fig. 3, bottom panels, red signal) and for the tumor marker carcinoembryonic antigen CEA, whose signal was visible either in intracellular spots or on the cell surfaces (Fig. 3, bottom panels, green signal).

For a quantitative evaluation of the ability of the two cancer cell lines (AGS and Caco2 cells) to adhere to different HPMC monolayers, we used the DiI tracer as above to mark the cancer cells before the adhesion test. For the analysis we utilized three primary cultures of mesothelial cells, derived from the peritoneal washes of patients without carcinoma disease (Fig. 4A), with colorectal cancer (Fig. 4B) or

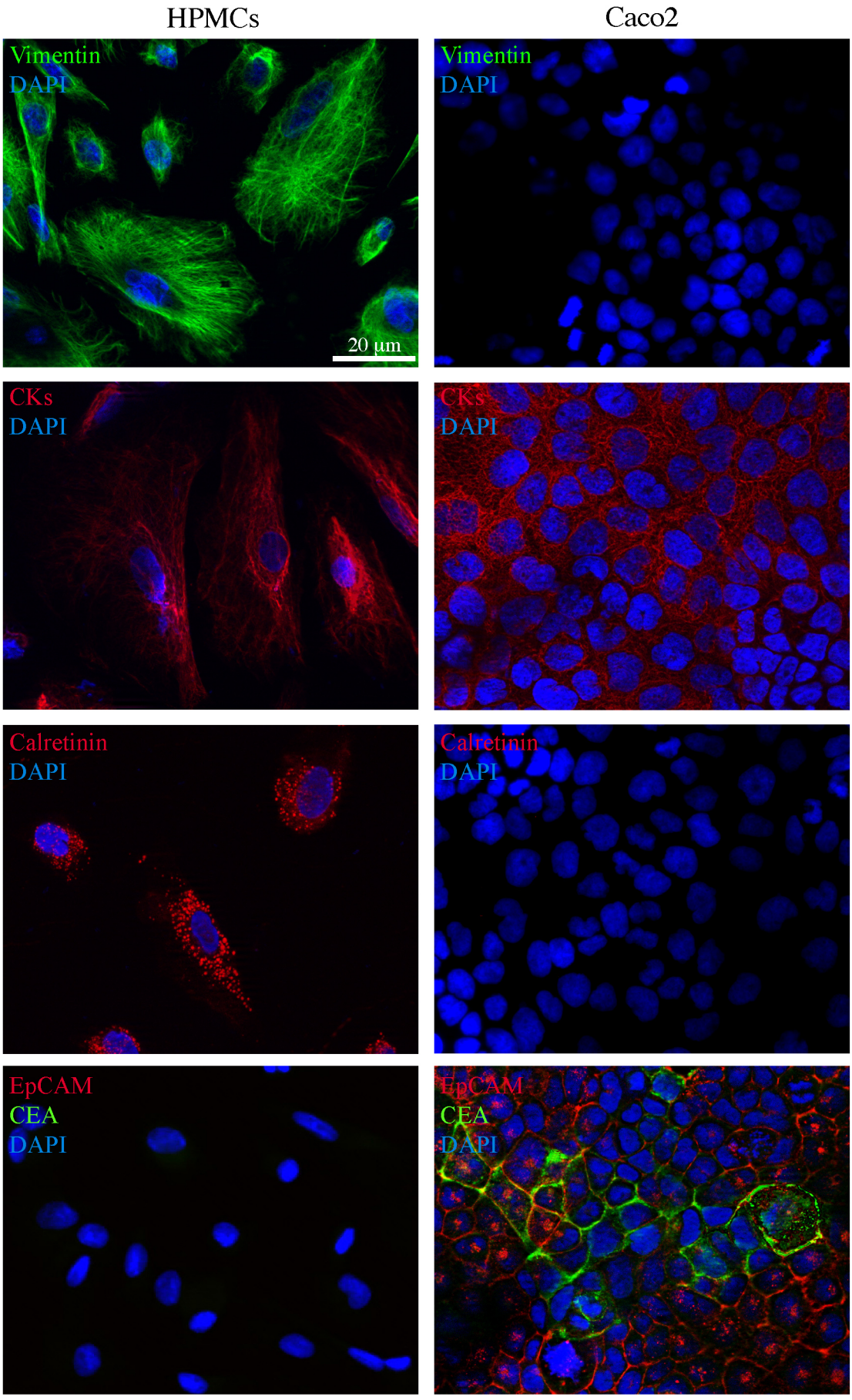
HPMCs
Caco2
Vimentin
DAPI
20 μm
Vimentin
DAPI
CKs
DAPI
CKs
DAPI
Calretinin
DAPI
Calretinin
DAPI
EpCAM
CEA
DAPI
EpCAM
CEA
DAPI

Figure 3. Immunofluorescence characterization of human peritoneal mesothelial cells from peritoneal washes of gastric and colon cancer patients.
Primary cultures of human peritoneal mesothelial cells (HPMCs) were isolated from peritoneal washes as described in materials and methods. Caco2 colon cancer cells were used as a control. Immunofluorescence analysis using antibodies directed against mesothelial (vimentin, CK8 and CK19 cytokeratins and calretinin) and epithelial (EpCAM and CEA) markers shows that HPMCs are positive for vimentin and cytokeratin staining, that appears as perinuclear bundles of filaments, as well as for the hot-spotted calretinin signal, but are negative for the plasma membrane EpCAM staining and for the intracellular and surface CEA signal. Caco2 cells are positive for cytokeratins and double positive for the EpCAM and CEA epithelial markers visible on the cell surfaces (EpCAM, green signal) or on the plasma membranes and in intracellular spots (CEA, red signal). Nuclei were stained with DAPI. Bar: 20 μm

with gastric cancer (Fig. 4C) and we were able to compare the contribution of different mesothelial monolayers to the adhesion of the same type of cancer cells at different time points (1, 24 and 48 hours). The quantitative analysis of the adhesion of DiI+ cells to the HPMC monolayers (Fig. 4A-C) showed reduced levels of adhesion in timespan for both tumor cell lines compared to the adhesion test performed on MeT-5A (see Fig. 2B). On these primary cultured monolayers, the Caco2 cells were more adherent than AGS cells at either 24 or 48 hours, independently on the origin of the peritoneal washes. However, while the adhesion of the Caco2 cells was comparable to all mesothelial layers, irrespectively on their source from patients with neoplastic or benign disease, the AGS cells display significant differences in their behaviour, showing higher adhesion to the HPMCs from colon cancer patient (#062) respect to the HPMCs from either gastric cancer patient (#210) or from non-carcinoma disease (#Ctrl2). Thus, while the adhesion properties of the mesothelial monolayers appear independent on the cancer environment, our co-culture model is able to detect differences among the HPMCs.

2.3.3 Role of HPMC senescence in the adhesion process

To analyze by our model the contribution of possible cellular and molecular mechanisms which may play a role in the different adhesive properties of the HPMCs, we focused our attention on the mesothelial senescence. In fact, among the physiological characteristics of the mesothelial monolayer, the senescence level of

HPMCs is believed to promote the adhesion of tumour cells (Ksiazek et al., 2008, 2009, 2010). Interestingly, our HPMCs, being derived from peritoneal washes instead of from omentum samples, displayed already at the first in vitro passage the well known features of senescence, like an enlarged morphology, multiple nuclei and cytoplasmic vacuolization (Yung et al., 2006). Because it has been proposed that the peritoneal senescence correlates with an increase of the expression of the intercellular adhesion molecule 1 (ICAM1) on the plasma membrane as a consequence of the oxidative stress (Ksiazek et al., 2010), we wondered if we could observe differences in ICAM1 expression in our selected HPMCs. To this purpose, we evaluated by quantitative immunofluorescence the percentage of ICAM1 positive cells in HPMC monolayers after the first confluence comparing the three representative cultures used above: the HPMCs from colon cancer patient (#062), which appeared to better contribute to the adhesion of the cancer cells in the experiments described above (Fig. 4), showed an higher percentage of ICAM1 positive cells respect to the other mesothelial cells (Fig. 5A).

In addition, since in the study of Ksiazek et al. (Ksiazek et al., 2009) senescence of human omentum-derived peritoneal mesothelial cells was induced in vitro to analyze its effect on tumour cell adhesion, we applied a similar approach inducing the senescence of our primary cultures by sequential passaging.

To this aim, we compared the same primary culture of HPMCs from colon cancer patient at two different passages: P2, obtained by seeding after the first confluence, and P4, after 2 passages 1:3 from P2, as reported (Ksiazek et al., 2009). The phase

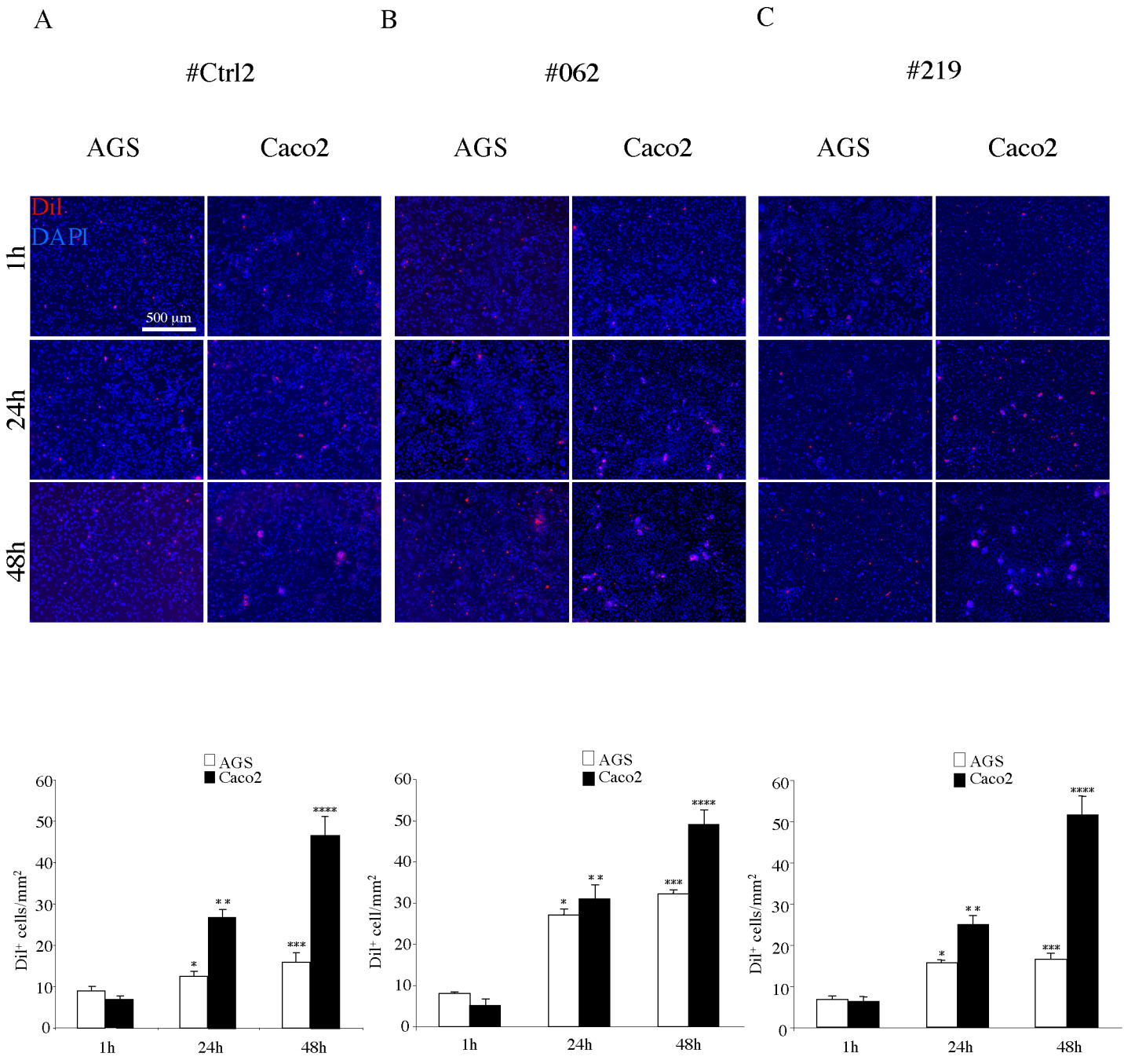
A
B
C
#Ctrl2
#062
#219
AGS
Caco2
AGS
Caco2
AGS
Caco2
1h
24h
48h
DiI
DAPI
500 µm
AGS
Caco2
Dil+ cells/mm2
Dil+ cell/mm2
0
10
20
30
40
50
60
1h
24h
48h
*
**
***
****

Figure 4. Adhesion test with AGS and Caco2 cells on different HPMC monolayers.

HPMCs isolated from the peritoneal wash of a non-cancer patient (A, #Ctrl2), from that of a colon cancer patient (B, #062) and from that of a gastric cancer patient (C, #219), were grown to confluent monolayer as above. Caco2 and AGS cells were labeled with Dil, seeded on the HPMC layers, left to adhere for different time points (1, 24 and 48 hours) and then washed, fixed and permeabilized. Nuclei were stained with DAPI. Quantitative analysis of the number of adherent Dil+ cells/mm2 was performed as described in materials and methods. Independently on the origin of the peritoneal washes, the Caco2 cells show higher levels of adhesion respect to AGS at 24 and 48 hours. However, while the adhesion of the Caco2 cells is similar to all mesothelial layers, the AGS cells display significant differences, showing higher adhesion to the layer #062 respect to the #219 and the #Ctrl2.

Results of the quantitative analysis are expressed as mean values ± IC 95%. Kruskal-Wallis test: A) *$p<0.05$ vs the AGS 1 hour; **$p<0.01$ vs Caco2 1 hour, $p<0.01$ vs AGS 24 hours; ***$p<0.05$ vs the AGS 1 hour and p=NS vs the AGS 24 hours; ****$p<0.01$ vs Caco2 24 hours. B) *$p<0.01$ vs the AGS 1 hour; **$p<0.01$ vs Caco2 1 hour, p=NS vs AGS 24 hours; ***$p<0.05$ vs the AGS 1 hour, p=NS 24 AGS hours; ****$p<0.01$ vs Caco2 24 hours. C) *$p<0.01$ vs the AGS 1 hour; **$p<0.01$ vs Caco2 1 hour, $p<0.01$ vs AGS 24 hours; ***$p<0.05$ vs the AGS 1 hour, p=NS 24 AGS hours; ****$p<0.001$ vs Caco2 24 hours.

contrast microscopic analysis showed an increase in the cell size and in the number of vacuolated cells (Fig. 5B, arrowheads), reflecting the increase in the level of senescence from P2 to P4. In addition, because peritoneal senescence correlates with an increase of the expression of the intercellular adhesion molecule 1 on the plasma membrane as a consequence of the oxidative stress (Ksiazek et al., 2010), we confirmed the induction of senescence in our cultures by quantitative immunofluorescence with anti-ICAM1 antibodies (Fig. 5B): the results demonstrated that either the percentage of ICAM1-positive cells or the fluorescence intensity of the ICAM1 signal on the cell surface, assessed as described in materials and methods, were clearly increased from passage P2 to P4. The ICAM1-positive cells were larger than the negative cells in the same culture and frequently apperead multinucleated and vacuolated as observed also in the corresponding phase contrast images (Fig. 5B), further demonstrating that HPMCs at P4 were more senescent respect to P2.

For an additional assessment of the senescence levels, we investigated the oxidative state of our P2 and P4 cultures evaluating the intracellular production of reactive oxigen species (ROS). To this purpose, we performed a test based on the addition of DCFH-DA (2',7'-dichlorofluorescein diacetate) and fluorescence detection by confocal microscopy and we compared the levels of ROS production in P2 and P4 cultures: as shown in figure 5C, the results obtained by the quantitative fluorescence analysis, performed as described in materials and methods, were

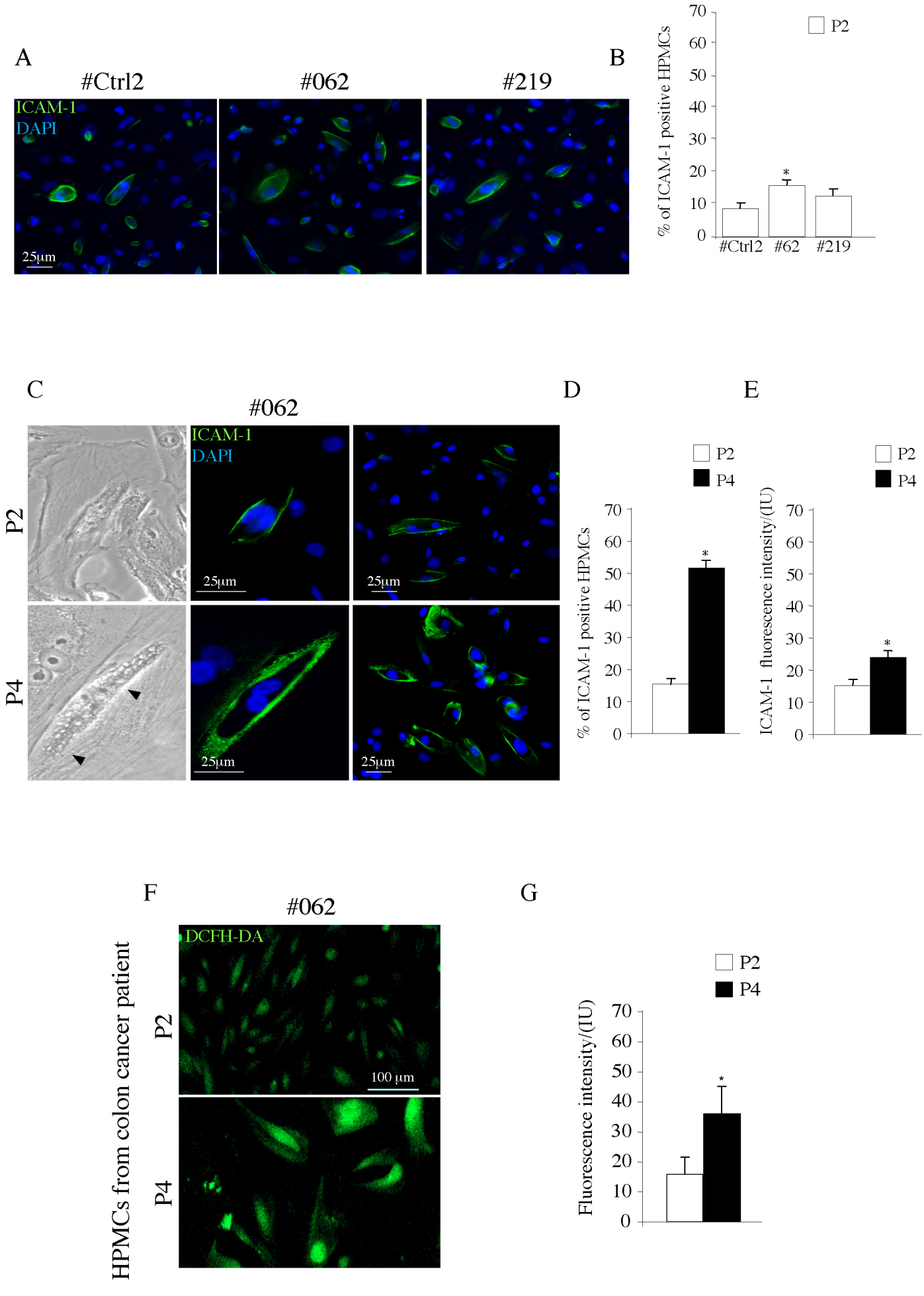
A
#Ctrl2
#062
#219
ICAM-1
DAPI
25µm
B
P2
% of ICAM-1 positive HPMCs
70
60
50
40
30
20
10
0
*
#Ctrl2
#62
#219
C
#062
P2
P4
ICAM-1
DAPI
25µm
D
P2
P4
% of ICAM-1 positive HPMCs
*
E
P2
P4
ICAM-1 fluorescence intensity/(IU)
*
F
#062
HPMCs from colon cancer patient
P2
P4
DCFH-DA
100 µm
G
P2
P4
Fluorescence intensity/(IU)
*

Figure 5. Expression of ICAM1 and intracellular ROS production in HPMC monolayers during in vitro induced senescence.

A) Quantitative evaluation of the percentage of ICAM1 positive cells in HPMC monolayers from the peritoneal wash of the non-cancer patient (#Ctrl2), from that of the colon cancer patient (#062) and from that of the gastric cancer patient (#219) after the first confluence (P2). The HPMCs from the colon cancer patient shows an higher percentage of ICAM1 positive cells respect to the other mesothelial cells. Results are expressed as mean values ± SE. Kruskal-Wallis test: *p<0,01 vs #Ctrl2 and p<0,05 vs #219.

B) Phase contrast microscopy (left panels) of #062 cultured at different passages to induce senescence: size enlargement and increase of vacuolated cells (arrowheads) from passage 2 (P2) to passage 4 (P4) confirm the enhanced level of senescence of P4.. Bars: 25 μm. The quantitative analysis of the percentage of ICAM1 positive cells in P2 and P4 passages shows the increase in the percentage of positive cells from P2 to P4. Quantitative immunofluorescence analysis with anti-ICAM1 antibodies shows that both the number of ICAM1 positive cells, displaying a clear plasma membrane staining, and the fluorescence intensity of the signal are increased in P4 cultures respect to P2 HPMCs. The parallel phase contrast observations show that the ICAM1 positive cells are enlarged and vacuolated as expected for senescent cells. The cellular nuclei were stained with DAPI. Results in the first graph are expressed as mean values ± SE. Kruskal-Wallis test: *p<0,001 vs P2. The quantitative evaluation of the fluorescence intensity of the ICAM1 signal was performed as described in materials and methods: results in the second graph are expressed as mean values ± IC 95%. Student's t test: *p<0,01 vs P2.

C) Evaluation of ROS production in HPMCs at P2 and P4 passages was performed with addition of DCFH-DA (2',7'-dichlorofluorescein diacetate) and fluorescence detection by confocal microscopy as described in materials and methods. The increase in the fluorescence intensity signal of DCFH-DA in the late passage P4 compared with the earlier P2 confirm the enhancement of ROS generation induced by senescence of the mesothelial cells. Results are expressed as mean values ± SE. Student's t test: *p<0,001 vs P2.

consistent with an increase of fluorescent cells in the P4 late passage compared with the P2 early one, in agreement with the literature (Ksiazek et al., 2009).

To determine if the different levels of senescence could affect the adhesion of the cancer cells to the mesothelial monolayers, we evaluated, through the in vitro test used above, the ability of the Caco2 cells to adhere to the cultures of HPMCs at the different passages, P2 and P4. The results obtained by the contemporary use of DiI and DAPI staining of the co-cultures at various time points (1h, 24h, 48h) from seeding, showed a significant increase in the number of cancer cells adhering to the late P4 respect to the early P2 passages (Fig. 6A and 6B). To ascertain the possible involvement of the enhanced ICAM1 expression of the senescent cells in increasing the adhesion, we added decreasing dilutions of an anti-ICAM1 blocking antibody during the time course of the adhesion test: the antibody addition led to a progressive dose-dependent inhibition of the cancer cell adhesion (Fig. 6C), revealing that the ability of the cancer cells to better interact with senescent HPMCs is related to the increased expression of ICAM1 on the cell plasma membranes of the mesothelial cells, as reported (Alkhamesi et al., 2005; Ksiazek et al., 2010).

2.4 Discussion and conclusions

The role of the mesothelial cells in the process of cancer spreading in the peritoneal cavity has been, up to now, underestimated and remain to be clarified. However, similarly to the emerging crucial contribution of the stromal microenvironment

A

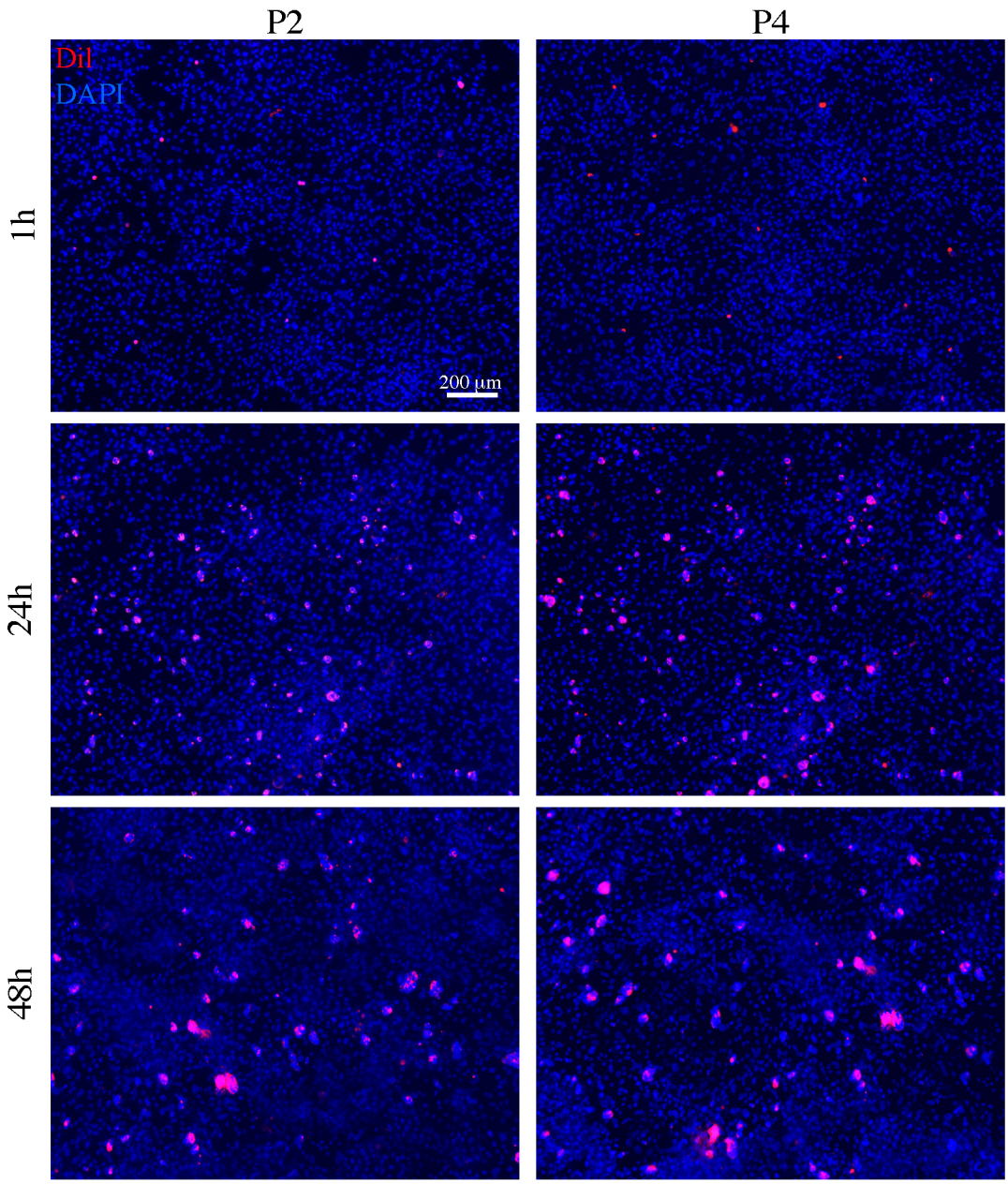
#062
P2
P4
DiI
DAPI
1h
24h
48h
200 µm

B

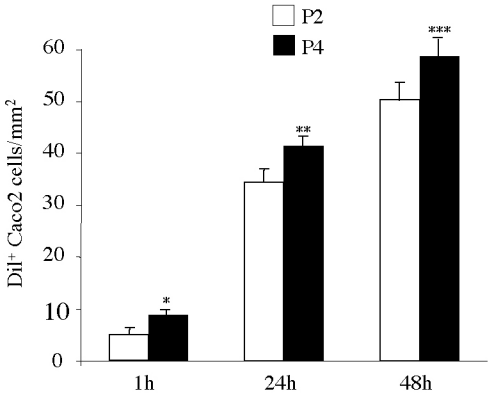
P2
P4
Dil+ Caco2 cells/mm2
60
50
40
30
20
10
0
*
**
***
1h
24h
48h

C

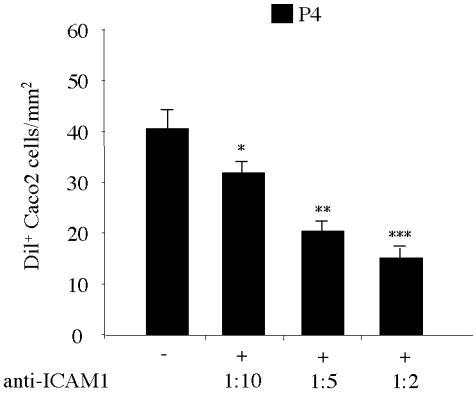
P4
Dil+ Caco2 cells/mm2
60
50
40
30
20
10
0
*
**
***
-
+
1:10
+
1:5
+
1:2
anti-ICAM1

Figure 6. Adhesion test with Caco2 cells on senescent HPMC monolayer.
A) HPMCs from the #062 peritoneal wash were cultured at P2 and P4 as described in figure 5. Caco2 cells were labeled with Dil, seeded on the HPMC layers, left to adhere for different time points (1, 24 and 48 hours) and then washed, fixed and permeabilized. Nuclei were stained with DAPI.
B, C) Quantitative analysis of the number of adherent Dil+ cells/mm2 was performed as described in materials and methods. In B, the number of cancer cells adhering to the HPMC monolayer at P4 is significantly increased respect to the values in P2 at all time points. In C, the addition of decreasing dilutions of an anti-ICAM1 blocking antibody at the representative 24 hours time point leads to a progressive dose-dependent inhibition of the cancer cell adhesion to HPMCs at P4. Results in B are expressed as mean values ± SE. Kruskal-Wallis test: *p<0,05 vs the P2 at 1 hour; **p<0,05 vs the P2 at 24 hours; ***p<0,05 vs the P2 at 48 hours. Results in C are expressed as mean values ± SE. Kruskal-Wallis test: *p<0,05 vs the absence of blocking antibody; **p<0,01 vs the antibody dilution 1:10; ***p<0,05 vs the antibody dilution 1:5.

surrounding the tumor tissue in the neoplastic progression, also the peritoneal layer is expected to represent a key mediator in the development of the carcinomatosis. The molecular mechanisms which may affect the interaction of the epithelial cancer cells to the mesothelium are probably quite analogous to those controlling the tumor cell adhesion to the endothelial layer during metastatic dissemination: both the fibrinolytic activity and the pattern of expression in adhesion molecules on the mesothelial or endothelial cells are major players in the process (Celeen et al., 2009; Ivarsson et al., 1998). In this paper, with the aim to investigate how the behaviour of mesothelial cells may differ depending on the tumor context of their origin as well as the possible state of activation or senescence, we propagated in vitro HPMCs isolated from different peritoneal washes of patients affected by colon or gastric cancers or from patients with benign diseases: in fact, the isolation of the mesothelial cells from the lavages, instead of from omental fragments, permits to obtain primary cultures resembling more closely the in vivo conditions, as suggested (Ivarsson et al., 1998). Consistent with what has been previously reported (Yung et al., 2006), we found that our primary cultures displayed all the morphological features and the marker positivity (CK8, CK19 and calretinin) characteristic of the mesothelial cells.

For the adhesion test, we selected and optimized a co-culture method, previously proposed for ovarian cancer cells (Heyman et al., 2008), based on the quantitative analysis of the adhesion of DiI+ cells to the HPMCs. First we set up the test using the mesothelial cell line MeT-5A and, when we moved to the primary cultures, we

found reduced levels of adhesion of the cancer cells at all time points compared to the adhesion obtained with the MeT-5A monolayer, in agreement with the observations reported by Heyman et al. (Heyman et al., 2008) utilizing the same DiI-based test. Our results with the HPMC layers, showing that both the AGS gastric carcinoma cells and the Caco2 colon carcinoma cells did not change their adhesion and growth when seeded on different mesothelial monolayers, indicated that the adhesive behaviour of the cancer cells was not affected by the origin and possible activation state of the HPMCs associated with different cancers.

To demonstrate that our cultures of HPMCs from peritoneal washes would represent a more reliable model of adhesion respect to other previously proposed with HPMCs from other sources, we first analyzed their expression of ICAM1, since this adhesion molecule is known to be more elevated in HPMCs from peritoneal wash comparing with cells from omental biopsies (Sikkink et al., 2009) and it has been recently reported that the increase in ICAM1 expression promotes the adhesion of cancer cells (Alkhamesi et al., 2005; Ksiazek et al., 2010). In agreement with the reported observations (Sikkink et al., 2009), our primary cells showed an high expression of ICAM1 at early passages of the culture, suggesting that these detached cells present in the peritoneal fluid in vivo may possess adhesive properties more pronounced respect to the peritoneal intact layer. Interestingly, the HPMCs from peritoneal washes analyzed in our study were characterized also by the typical features of senescence already at the first in vitro P2 passages and by quite high levels of basal ROS production. Further increase of

these features, i.e. ICAM1 expression and ROS generation, were obtained inducing in vitro senescence, as expected (Ksiazek et al., 2008, 2009, 2010). These acquired senescent state led to an increase in the adhesion of the cancer cells, which was inhibited by the addition of serial dilutions of a blocking anti-ICAM1 antibody, strengthening the role of ICAM1 in the adhesion process and suggesting that this ICAM1-mediated molecular interaction might be even more crucial for cells floating in the peritoneal fluid from which our cultures are derived.

In conclusion, we suggest that the cancer environment might be not crucial for the peritoneal dissemination. However, we propose that the use of HPMCs from peritoneal washes would provide a practical and reliable tool for the in vitro analysis of the mesothelial molecular pathways involved in the adhesion process, the evaluation of the mesothelial conditions in cancer patients and the selection or validation of possible therapeutic strategies.

3. Clinical relevance of free peritoneal tumor cells detection in gastric and colorectal cancer.

3.1 Aims

In the attempt to further demonstrate the diagnostic/prognostic value of the detection of epithelial-tumor markers in the peritoneal washes and to rule out the possibility of false positive results using molecular-based techniques alone, in this study we combined the qRT-PCR analysis with an immunomagnetic enrichment followed by immunofluorescence (IF) analysis, for enhancing the specificity of detection of the free peritoneal tumor cells (FPTCs). To this aim, the peritoneal washes were directed to a procedure commonly used for detection of circulating tumor cells CTC from blood samples (Gervasoni et al., 2008). To detect the disseminated epithelial cells, we used monoclonal antibody against the pan-epithelial marker EpCAM/CD326 and to ascertain their tumor origin we used polyclonal antibodies against the carcinoembryonic antigen (CEA). In this setting, IF microscopy allowed the morphological assessment and unequivocal identification of the FPTCs as well as validation of the molecular analysis. This combined use of immunomagnetic enrichment, IF analysis and real-time qRT-PCR, showing a greater sensibility respect to conventional cytology, was able to permit the detection of free peritoneal tumor cells in both gastric and colorectal cancer and to determine their prognostic value for survival.

3.2 Materials and methods

3.2.1 Patients and Surgery

All patients were extensively informed and gave written consent for the investigations. The study was approved by the local ethical commission. Twenty-seven gastric and 48 colorectal patients with cancer who underwent surgery between December 2008 and December 2009 at the A Unit of Surgery of Sant'Andrea Hospital were investigated.

Patients with distal extraperitoneal rectum cancer were excluded from the study. Preoperative chemotherapy or radiation therapy was not performed in this series.

Gastric cancer patients (GC) underwent subtotal gastrectomy in 15 cases, total gastrectomy in 8 cases and palliative surgery in 4 cases.

Colorectal cancer patients (CRC) underwent right colectomy in 23 cases, left colectomy in 10 cases, anterior resection in 14 cases and palliative surgery in 1 case. All patients underwent open surgery.

A control group comprised 6 patients with a variety of non-carcinoma diseases: benign uterus tumor, cholecystolithiasis and colic adenoma. Follow-up data were obtained for a median observation time of 17 months (range 1-27 months).

3.2.2 Samples

Immediately after a midline abdominal incision had been made and before manipulation of the tumor, peritoneal washing was performed. Intraoperatively,

250 mL of saline were instilled into the abdominal cavity over the tumor site and at least 150 mL were reaspirated. Twenty mL were sent for cytological examination which was performed after Papanicolaou and Giemsa stainings. The slides were examined by light microscopy by experienced cytologists unaware of the clinical findings. Patients with suspicious morphological evidence of malignancy by microscopy were included in the positive cytology group.

3.2.3 RNA extraction and cDNA synthesis

Each peritoneal wash sample was centrifuged at 1200 rpm for 10' and total RNA was extracted using the TRIzol method (Invitrogen, Carlsbad, CA, USA) according to the manufacture's procedure. Briefly cells were homogenized in 1 mL TRIzol reagent and RNA was extracted by incubation and centrifugation in 0,2 mL $CHCl_3$. RNA was precipitated from aqueous phase by 0,5 mL of isopropanol. RNA pellet was washed in 75% ethanol and eluted with 0,1% diethylpyrocarbonate (DEPC)-treated water.

Total RNA quantity, purity and absence of ribonuclease digestion were assessed by measuring the optical density ratio 260/280 nm. Total RNA samples were stored at -80°C. After denaturation in DEPC-treated water at 70°C for 10 min, 1 μg of total RNA was used to cDNA synthesis using cDNA synthesis mix (Bio-Rad Laboratories, Hercules, CA, USA).

3.2.4 Real-time PCR primer design

Gene sequences were obtained from the NCBI database. Oligonucleotide primers for CEA and CK20 target genes and GAPDH housekeeping gene were chosen with the assistance of the Beacon Designer 7.0 computer program (Bio-Rad Laboratories). The primers sequences used throughout this study are described in the Table 2. For each primer pair, we performed no-template control and no-reverse-transcriptase control (RT negative) assays, which produced negligible signals (usually >45 in threshold cycle (Ct) value), suggesting that primer dimer formation and genomic DNA contamination effects were negligible. Oligonucleotide primers were purchased from Invitrogen.

3.2.5 PCR amplification

Real-time PCR was performed using the iCycler Real-Time Detection System (iQ5 Bio-Rad) with optimized PCR conditions. The reaction was carried out in a 96- well plate using iQ SYBER Green Supermix 2X (Bio-Rad) adding each forward and reverse primers and 1 µl of diluted template cDNA to a final reaction volume of 15 µl. All assays included a negative control and were replicated three times. The relative expression of GAPDH was used for standardizing the reaction. The thermal cycling conditions comprised an initial denaturation step at 95°C for 3 minutes, followed by 45 cycles at 95°C for 10 seconds and 60°C for 30 seconds.

name	Primer Forward	Primer Reverse	Eff.%
GAPDH	5′CATCAGCAATGCCTCCTGCAC3′	5′GTCATGAGTCCTTCCACGATACCAA3′	99.7
CEA	5′AGGACAGAGCAGACAGCAGAG3′	5′GGTTCCAGAAGGTTAGAAGTGAGG3′	94.4
CK20	5′TGCTACTTACCGCCGCCTTC3′	5′CCTTGCCATCCACTACTTCTTGC3′	103

Table 2. Primers sequence and amplification efficiency.

3.2.6 Data analyses

Real-time quantitation was performed by using SYBR Green dye as fluorescent signal, with the help of the iCycler IQ optical system software version 3.0a (Bio-Rad), according to the manufacturer's manual. Quantitative values are obtained from the Ct number at which, the increase in signal associated with exponential growth of PCR products, starts to be detected. Target genes (CEA, CK20) amplification was compared with simultaneous amplification of an endogenous reference gene (GAPDH) and each sample was normalized on the basis of its GAPDH content.

The target genes CEA and CK20 were tested for expression in tenfold serial dilutions (10^6-10^0) of cancer cell lines from colon (HT29, Caco2) and gastric (AGS) carcinoma. Normal human fibroblast cell line from colon (CCD18) and primary culture of human fibroblasts from skin were used as negative controls.

For data analysis, receiver-operating characteristic (ROC) curves were used to compare the accuracies of CEA/GAPDH, CK20/GAPDH ratio and determine the cut off value by plotting sensitivity/specificity pairs for the two mRNA ratio. The clinical value of CEA and CK20 detection was assessed based on the diagnostic data from patients with positive cytology made at laparoscopy and from patients of the control group. The cut off value for CEA and CK20 was defined as 0.66 (gene target/GAPDH ratio). The sensitivity and specificity obtained at the determined

cut off were 77% and 100% respectively for the CEA/GAPDH ratio and 100% and 93% for the CK20/GAPDH ratio.

3.2.7 Immunomagnetic enrichment for epithelial cells

From each patient, 40 mL of peritoneal wash were collected in EDTA (50 μM). Samples were centrifuged at 1300 rpm for 6 min at 25°C and resuspended for magnetic labeling in 80 μL of MACS® separation buffer (Miltenyi Biotec, Bergisch Gladbach, Germany). Immunomagnetic depletion using anti-CD45 microbeads (Miltenyi Biotec) was performed according to the manufacturer's instructions to enrich for FPTCs (Figure 7A). Briefly, MS separation columns (MACS®, Miltenyi Biotec) had been equilibrated with 0,5 mL of MACS® separation buffer and the microbeads labeled cells were subjected to magnetic field trough the column passage. The CD45 negative cells were washed off from the column with 1,5 mL of MACS® separation buffer (Figure 7B) and centrifuged at 1300 rpm for 6 min at 25°C.

3.2.8 Immunofluorescence

CD45 negative cells were incubated with anti-CD326/EpCAM-FITC monoclonal Ab (1:10 in MACS® separation buffer) for 15 min at 4°C (Figure 7C). Cells were then washed, centrifuged at 1300 rpm for 6 min at 25°C and the pellet was

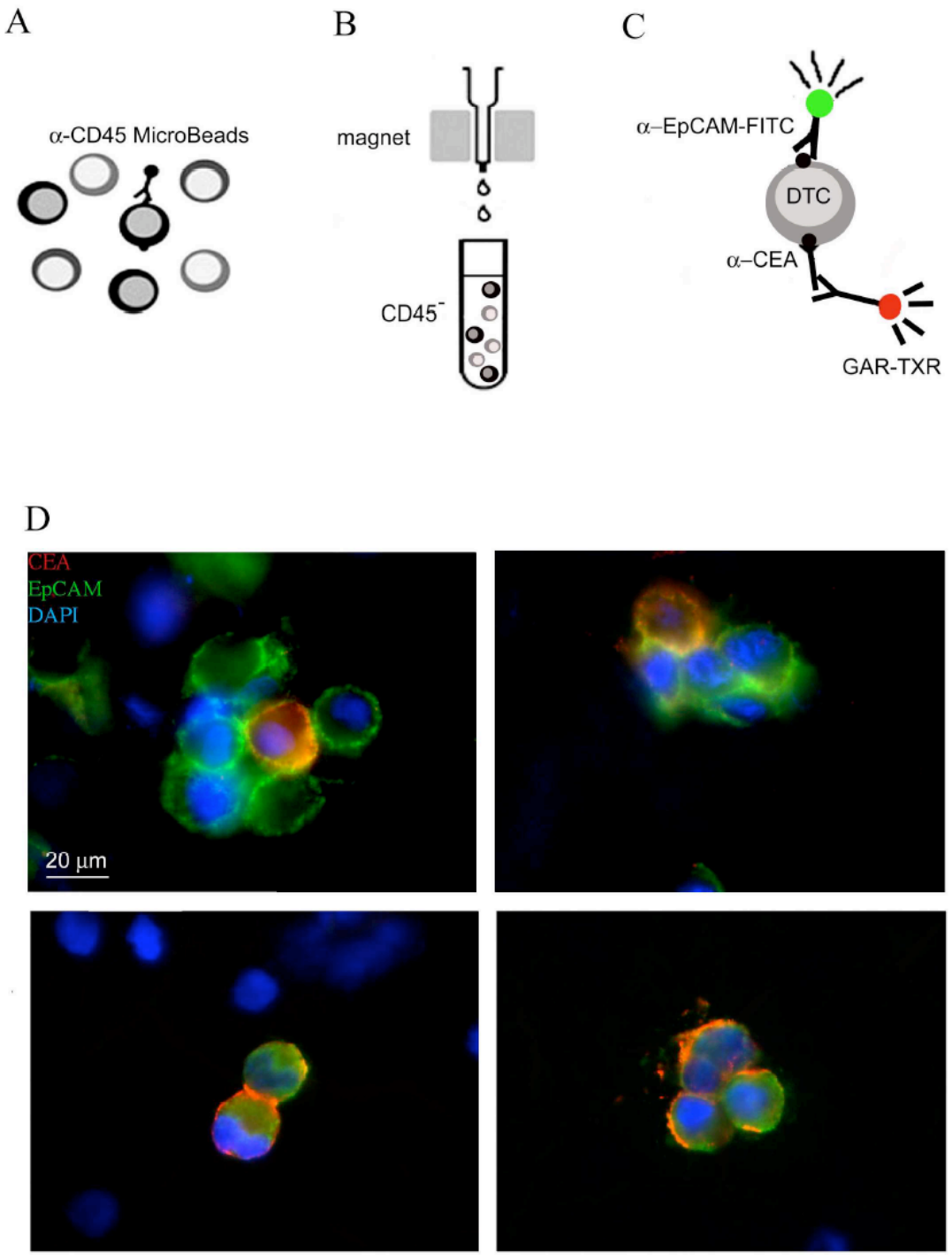

Figure 7: A-C. Immunoenrichment and immunofluorescence methods to detect free disseminated peritoneal tumor cells (see text). **D.** Images of EpCAM/CEA positive FPTCs (yellow) surrounded by epithelial cells positive for EpCAM (green) or IF double negative inflammatory or mesothelial cells.

resuspended in 10 μL of cell solution and spotted on 8 wells diagnostic slides (Menzel-Glaser, Braunschweig, Germany), left to dry and fixed with acetone for 8 min at -20°C. Cells were then incubated with anti-CEA polyclonal antibodies (Zymed, Invitrogen, Carlsbad, CA, USA) (1:100 in MACS® separation buffer) for 1 h at 25°C. After appropriate washing, the primary antibodies were visualized using goat anti-rabbit IgG-Texas Red (1:400 in MACS® separation buffer) for 30 min at 25°C. Nuclei were stained with DAPI (1 ng/mL, Sigma Chemicals, St Louis, MO, USA). Coverslips were finally mounted with mowiol for observation. Cells were analyzed by conventional fluorescence or by scanning in a series of 0.5 μm sequential optical sections with an ApoTome System (Zeiss, Oberkochen, Germany) connected with an Axiovert 200 inverted microscope (Zeiss). Image analysis was performed by the Axiovision software (Zeiss). Single optical sections were acquired by a CCD camera and image analysis was performed by the Axiovision software (Zeiss).

3.2.9 Statistics

A cross-tabulation analysis of histopathological findings with qRT-PCR analysis, immunofluorescence evaluation and cytologic examination was performed by the chi-square test for trend or Fisher's exact test.

The analysis of cancer specific survival and time to recurrence rates was calculated using the Kaplan-Meier method and compared using the log-rank test.

Cox proportional-hazards regression was performed to analyze the effect of all variables on survival and recurrence times.

A p value of 0.05 was considered as statistically significant.

3.3 Results

The application of immunomagnetic enrichment for epithelial cells and immunofluorescence analysis was performed in peritoneal lavages obtained from patients affected by gastric or colorectal cancers and this results were then associated and compared to the conventional cytology and to the molecular qRT-PCR analysis for the expression of CEA and CK20 mRNA.

For the immunomagnetic enrichment we used a consolidated method of immunodepletion of the inflammatory CD45+ cells, which are the major cell population present in the peritoneal washes. After depletion, the CD45- cells washed out from the column were immunolabeled for the epithelial marker CD326/EpCAM and for the tumor marker CEA: cells were then evaluated by immunofluorescence microscopy to search for the FPTCs (Figure 7A-C). In our analysis, only cells double positive for EpCAM and CEA were considered as FPTCs. In addition, careful observation of the cell nuclei stained by DAPI allowed to evaluate the cell viability and to exclude apoptotic or necrotic cells from our analysis (Fig 7D).

3.3.1 Relevance of free peritoneal tumor cells detection in gastric carcinoma

Global positivity rate for cytology, IF and qRT-PCR was 15%, 15% and 78% respectively. Cytology was positive in only 4 patients with T4 tumours, which were also characterized by massive peritoneal carcinomatosis. All these 4 patients were positive qRT-PCR markers and three of them were positive to the IF too. Interestingly, one patient with minor peritoneal carcinomatosis was negative at the cytological examination, but positive at both IF and qRT-PCR analysis. Table 3 shows the results for IF in gastric carcinoma patients. The chi-square test for trend showed how the worse grading (p=0.005), the deeper invasion of the gastric wall (p=0.01), the advanced stage of disease (p=0.014) and positive cytology (p=0.0014) are all related to the positivity at IF.

The molecular qRT-PCR method showed a remarkably higher incidence of positivity: in fact, expression of the markers was over the cut-off level in all T2 and T4 patients, in 3 out of 6 of the T1 patients and in 5 out of 8 of T3 patients. Moreover, as shown in Figure 8, there was a clear higher positivity for CEA (70%) respect to CK20 (41%). The combination of positivity for CEA and CK20 was observed in 36% of patients.

The positivity at qRT-PCR was not related to the depth of invasion, stage of disease and to the IF positivity but also associated to the worse grading (p=0.008; table 4).

The Kaplan-Meyer survival analysis showed how the positivity of IF and qRT-PCR for FPTCs was a statistically significant negative prognostic factor in both cancer

Factor	All patients	IF negative	IF positive	P value
No of patients	27	23 (85.2%)	4 (14.8%)	
Age (years)				
- mean ± SD	69.7 ± 12.8			
Gender				
- Male	14			
- Female	13			
Histology (differentiated/undifferentiated)				
- G1	2	2	0	0.005*
- G2	1	1	0	
- G3	18	18	0	
- G4	6	2	4	
Depth of invasion				
- T1	6	6	0	0.01*
- T2	5	5	0	
- T3	8	8	0	
- T4	8	4	4	
Stage at primary diagnosis				
- I	7	7	0	0.014*
- II	4	4	0	
- III	7	7	0	
- IV	9	5	4	
Cytologic examination				
- negative	23	23	0	0.0014^
- positive	4	1	3	

* Chi-square test for trend
^ Fisher's exact test

Table 3. Correlation between immunofluorescence evaluation, cytologic examination and histopathological findings in gastric carcinoma.

Factor	All patients	qRT-PCR negative	qRT-PCR positive	P value
No of patients	27	6 (22.2%)	21 (77.8%)	
Age (years)				
- mean ± SD	69.7 ± 12.3			
Gender				
- Male	14			
- Female	13			
Histology (differentiated/undifferentiated)				
- G1	2	2	0	0.008*
- G2	1	0	1	
- G3	18	4	14	
- G4	6	0	6	
Depth of invasion				
- T1	6	3	3	0.098*
- T2	5	0	5	
- T3	8	3	5	
- T4	8	0	8	
Stage at primary diagnosis				
- I	7	2	5	0.43*
- II	4	1	3	
- III	7	2	5	
- IV	9	1	8	
Immunofluorescence evaluation				
- negative	22	5	17	1^
- positive	5	1	4	

* Chi-square test for trend
^ Fisher's exact test

Table 4. Relationship between qRT-PCR analysis, immunofluorescence evaluation and histopathological findings in gastric carcinoma.

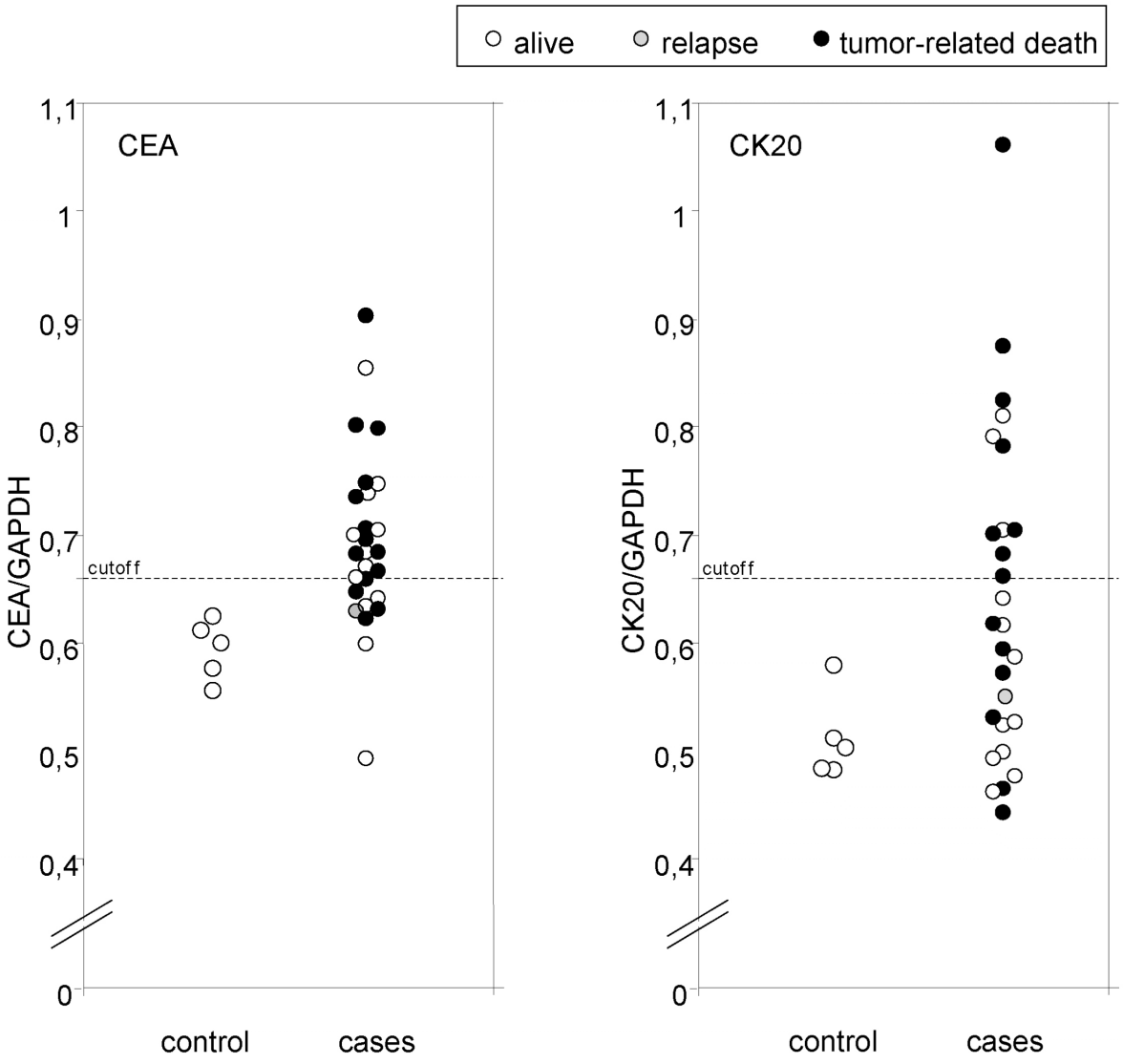

Figure 8. Expression levels of CEA and CK20 mRNA in control subjects and gastric cancer patients.

The cutoff values of CEA/GAPDH and CK20/GAPDH was 0.66. The open circles show the alive patients. The gray closed circles show patients who relapse. The black closed circles show patients who died by tumor-relates causes.

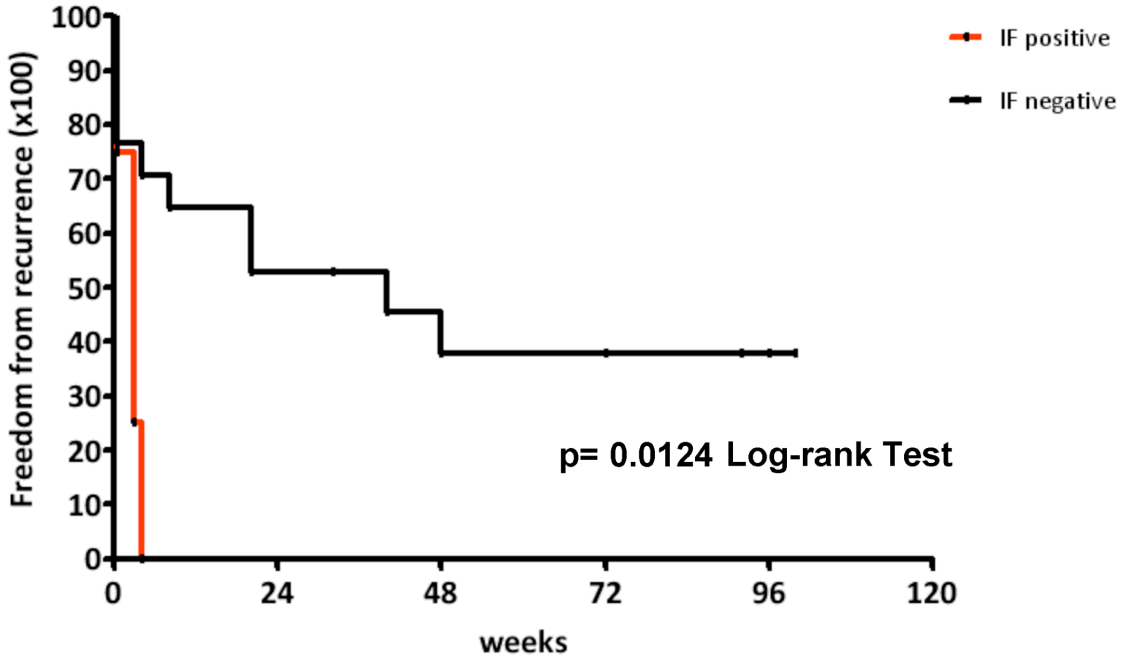

Figure 9. Time to recurrence rates by IF positivity in gastric cancer

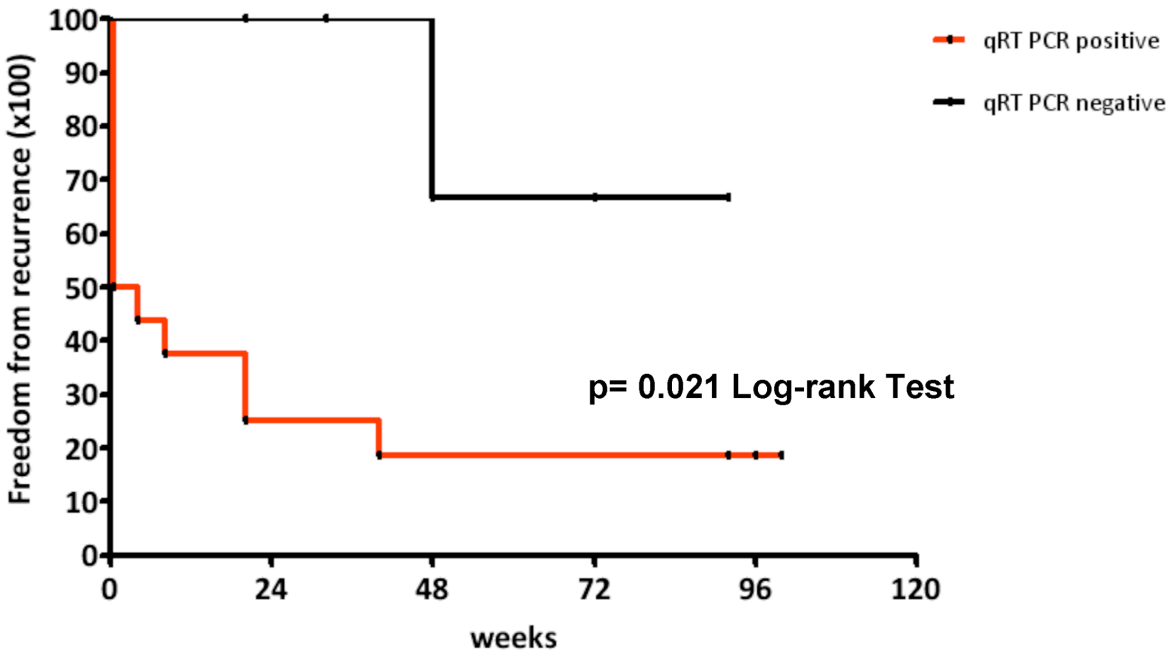

Figure 10. Time to recurrence rates by qRT PCR positivity in gastric cancer

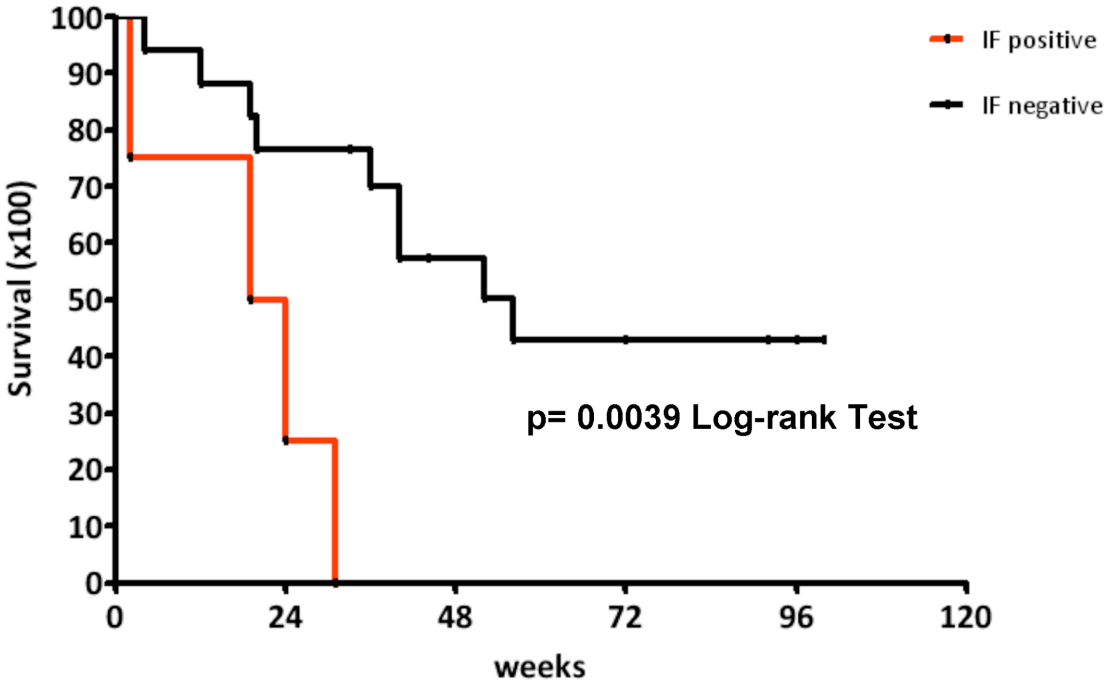

Figure 11. Cancer specific survival rates by IF positivity in gastric cancer

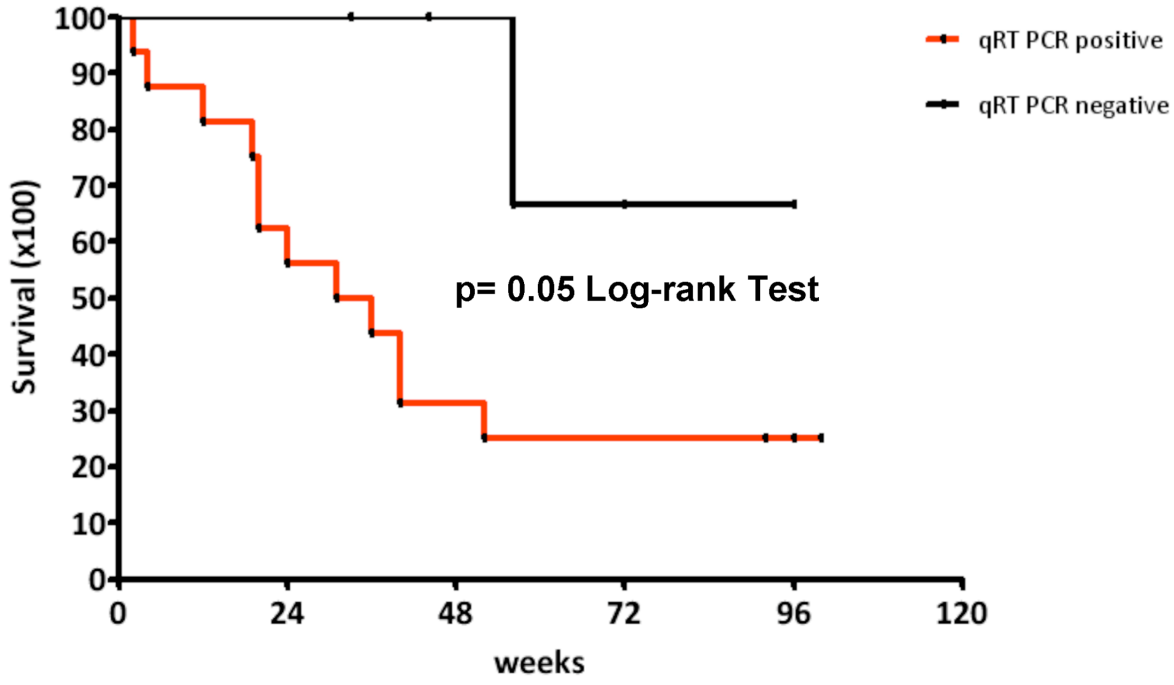

Figure 12. Cancer specific survival rates by qRT PCR positivity in gastric cancer

specific overall survival and disease free survival rates (Figures 9-12). At the multivariate analysis (Table 7), the stage at primary diagnosis was found to be an independent risk factor in overall survival only, while qRT-PCR resulted to be an independent risk factor in both overall and disease free survival with hazard ratio of 31.3 and 18.5 respectively ($p<0.05$). IF was found to be a statistically significant prognostic factor at univariate analysis (Figures 9 and 11), but it lost its prognostic power at multivariate analysis (Table 7).

3.3.2 Relevance of free peritoneal tumor cells detection in colorectal carcinoma

Global positivity rate for cytology, IF and qRT-PCR for FPTCs was respectively 0%, 17% and 42%. Cytology was negative in all patients, including one patient with peritoneal carcinomatosis; this same patient resulted positive for both CEA and CK20 at the qRT-PCR, but negative at IF. As shown in Table 6, IF was found positive in similar proportions in T2 (1/6 cases, 17%), T3 (5/27 cases, 19%) and T4 patients (2/14 cases, 14%). On the contrary of gastric carcinoma cases, posititive IF was not related to grading, depth of invasion and stage as shown in Table 5. In Table 6 are summarized the results for qRT-PCR: as well as the IF, no correlation was found between qRT-PCR and grading, depth of invasion and stage. Of the 8 patients who resulted positive to the IF, 7 of them were positive to qRT-PCR too, indicating a strong correlation between IF and PCR in colorectal carcinoma ($p=0.006$). As shown in Figure 13, there was a higher positivity for CEA (42%)

Factor	All patients	IF negative	IF positive	P value
No of patients	48	40 (83.3%)	8 (16.7%)	
Age (years)				
- mean ± SD	69.5 ± 12.3			
Gender				
- Male	22			
- Female	26			
Histology (differentiated/undifferentiated)				
- G1	1	1	0	0.13*
- G2	28	21	7	
- G3	16	15	1	
- G4	3	3	0	
Depth of invasion				
- T1	1	1	0	1*
- T2	6	5	1	
- T3	27	22	5	
- T4	14	12	2	
Stage at primary diagnosis				
- I	6	5	1	0.63*
- II	24	20	4	
- III	14	14	3	
- IV	4	4	0	
Cytologic examination				
- negative	48	40	8	-
- positive	0	0	0	

* Chi-square test for trend

Table 5. Correlation between immunofluorescence evaluation, cytologic examination and histopathological findings in colorectal carcinoma.

Factor	All patients	qRT-PCR negative	qRT-PCR positive	P value
No of patients	48	28 (58.3%)	20 (41.7%)	
Age (years)				
- mean ± SD	69.5 ± 12.3			
Gender				
- Male	22			
- Female	26			
Histology (differentiated/undifferentiated)				
- G1	1	1	0	0.57*
- G2	28	16	12	
- G3	16	10	6	
- G4	3	1	2	
Depth of invasion				
- T1	1	1	0	0.15*
- T2	6	4	2	
- T3	27	17	10	
- T4	14	6	8	
Stage at primary diagnosis				
- I	6	4	2	0.78*
- II	25	14	11	
- III	13	8	5	
- IV	4	2	2	
Immunofluorescence evaluation				
- negative	40	27	13	0.006^
- positive	8	1	7	

* Chi-square test for trend
^ Fisher's exact test

Table 6. Correlation between qRT-PCR analysis, immunofluorescence evaluation and histopathological findings in colorectal carcinoma.

respect to CK20 (10%). In addition, all patients positive for CK20 were also positive for CEA.

The analysis of survival was conducted on disease free survival only, due to the few tumor-related deaths occurred during the follow-up. Figured 14 and 15 shows the Kaplan-Meier survival curves for colorectal carcinoma patients: at Log-rank test worse prognosis was significantly associated to positive qRT-PCR ($p=0.018$) but not to IF ($p=0.88$). The multivariate Cox population analysis shows how qRT-PCR was found to be the only independent risk factor for relapse, with a hazard ratio of 6,95 ($p<0.05$; table 8).

3.3.3 Analysis of control patients

All samples of peritoneal lavage from the control group resulted negative for cytology, IF and real time qRT-PCR.

3.4 Discussion and conclusions

Peritoneal cytology has been introduced by many institutions as prognostic marker in both gastric and colorectal cancer. In gastric cancer its importance has been increasing during the last years and it has been proposed to use percutaneous or laparoscopic peritoneal lavage in the preoperative staging of patients (La Torre et al., 2010). Actually in some cases positive peritoneal cytology from patients with gastric cancer is being used as indication for neoadjuvant chemotherapy or as

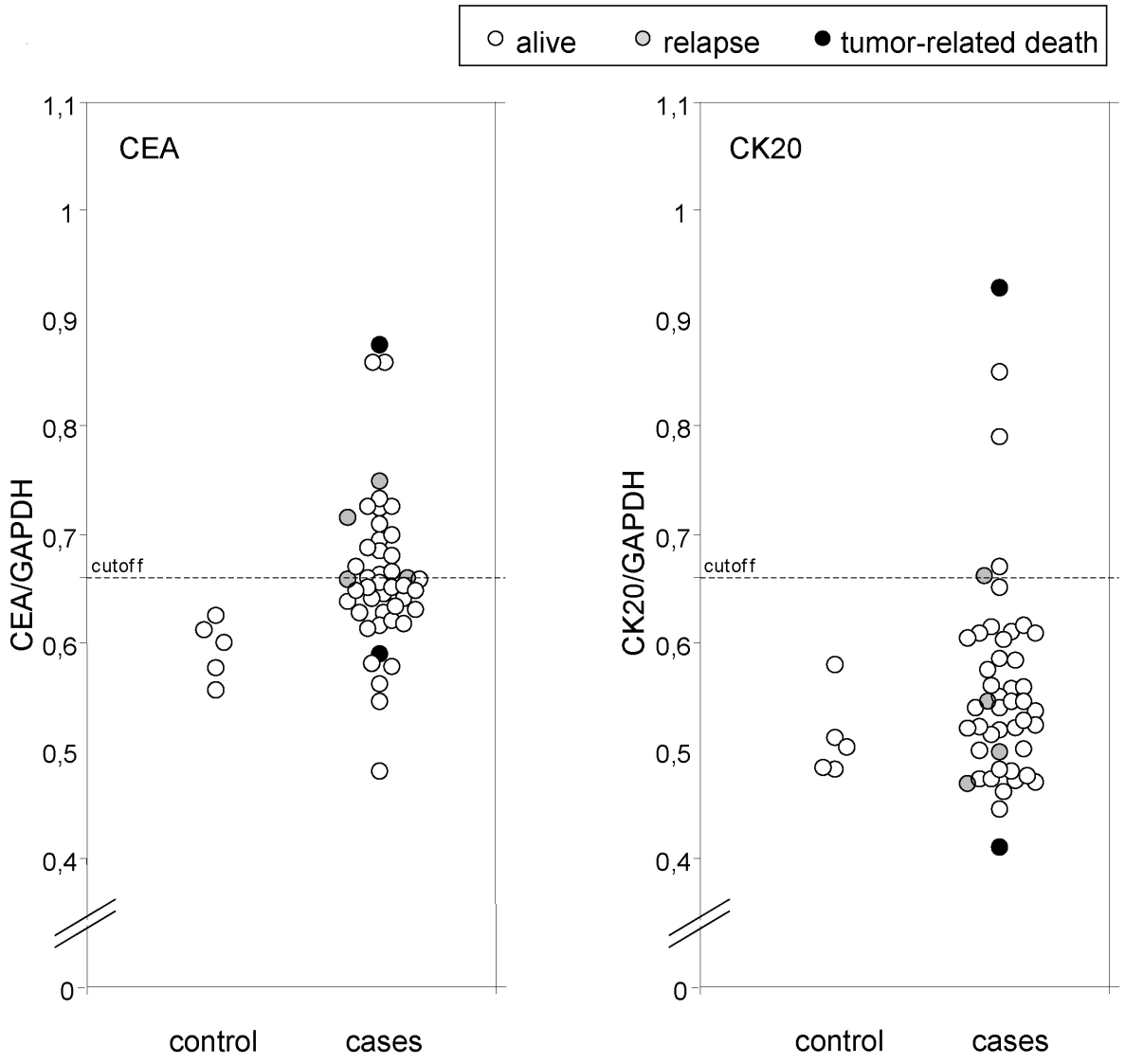

Figure 13. Expression levels of CEA and CK20 mRNA in control subjects and colorectal cancer patients.

The cutoff values of CEA/GAPDH and CK20/GAPDH was 0.66. The open circles show the alive patients. The gray closed circles show patients who relapse. The black closed circles show patients who died by tumor-relates causes.

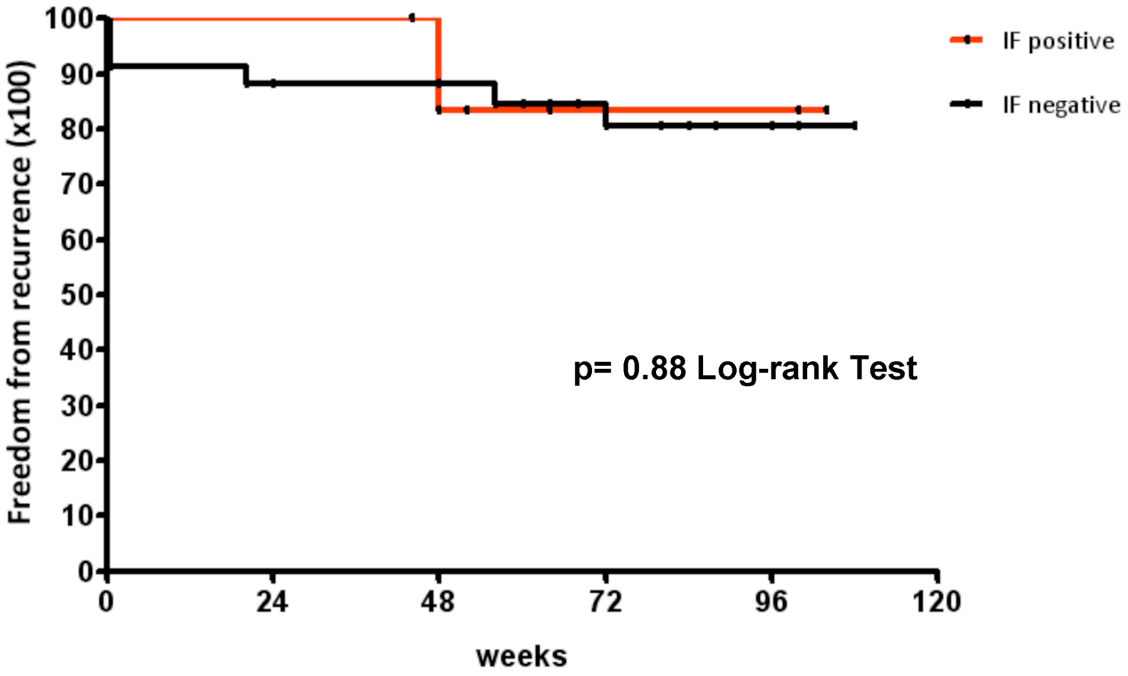

Figure 14. Time to recurrence rates by IF positivity in colorectal cancer

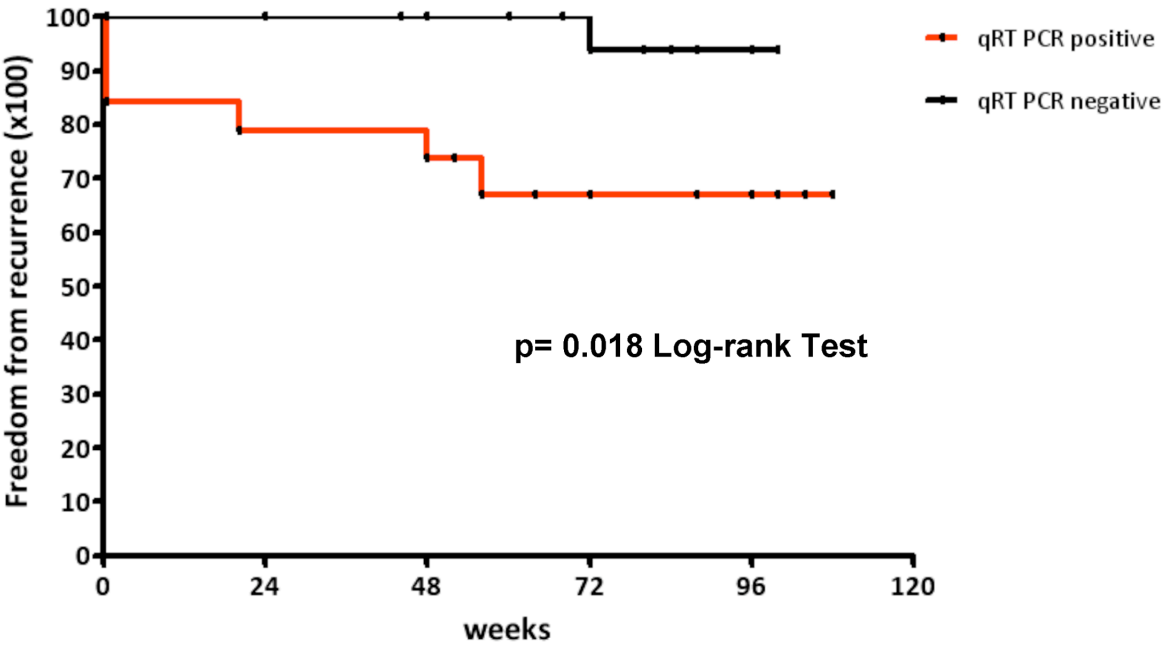

Figure 15. Time to recurrence rates by PCR positivity in colorectal cancer

	Progression-free survival		Overall survival	
	P-value	Hazard ratio (95% CI)	P-value	Hazard ratio (95% CI)
Depth of invasion				
T1-T3	0.13	1	0.65	1
T4		5.81 (0.56-59.7)		1.41 (0.31-6.29)
Histology				
G1-G2	0.28	1	0.14	1
G3-G4		0.15 (0.01-4.7)		0.04 (0.01-2.87)
Stage at primary diagnosis				
I-II	0.058	1	0.03	1
III-IV		9.08 (0.92-89.5)		11.9 (1.20-118.1)
IF evaluation				
negative				
positive	1	1	0.30	1
		1 (0.20-4.95)		2.49 (0.43-14.2)
qRT-PCR analysis				
negative	0.05	1	0.05	1
positive		18.5 (0.70-490.4)		31.3 (0.65-1494.7)

Table 7. Multivariate Cox population hazards analysis for the gastric cancer patients.

	Progression-free survival	
	P-value	Hazard ratio (95% CI)
Depth of invasion		
T1-T3	0.09	1
T4		4.84 (0.76-30.6)
Histology		
G1-G2	0.31	1
G3-G4		0.41 (0.07-2.32)
Stage at primary diagnosis		
I-II	0.17	1
III-IV		3.23 (0.59-17.7)
IF evaluation		
negative		
positive	0.90	1
		1.09 (0.18-6.46)
qRT-PCR analysis		
negative	0.05	1
positive		6.95 (0.78-61.4)

Table 8. Multivariate Cox population hazards analysis for the colorectal cancer patients.

absolute contraindication to surgery. It has been clearly assessed from many studies its value as negative prognostic marker: although positivity for peritoneal cytology increases with the stage of the disease, it has been found from different studies how its prognostic significance is independent. In fact, analyzing patients from the same stage of disease, those with positive peritoneal cytology had worse prognosis. The 7th TNM edition (Sobin LH, Gospodarowicz MK, Wittekind C. International Union Against Cancer (UICC) TNM classification of malignant tumours, 7th edition. New York: Wiley-Liss; 2010) has given great importance to peritoneal cytology, including in the M1 group those patients with positive washings even in absence of visible peritoneal implants.

In colorectal cancer the use of peritoneal cytology is less used and standardized than in gastric cancer, probably for the minor incidence of peritoneal carcinomatosis in this type of neoplasm. Most studies on patients affected with colorectal cancer show that the detection of single cancer cells in peritoneal cavity has prognostic relevance (Schott et al., 1998; Noura et al., 2009), but in other cases results were different (Wind et al., 1999).

The primary problems with conventional peritoneal cytology are the lack of sensitivity (positivity of 14-21% in gastric cancer and 0-11% in colorectal cancer) and the high operator-dependent feature of this test. In fact most of patients with positive peritoneal lavage develop peritoneal carcinomatosis, but it is even developed by many of the patients with negative peritoneal washing. Since the knowledge about the presence of isolated tumor cells in the peritoneal cavity has

been growing in importance for the treatment strategy in both gastric and colorectal cancer, clinicians need new and more sensitive and specific techniques to retrieve these new prognostic factors. The simplest technique that gives little advantage on the results of traditional cytopathology is to integrate it with immunocytochemical methods, using monoclonal antibodies directed to gastric cancer-associated antigens (Benevolo et al., 1998).

Kodera et al. (Kodera et al., 2002) proposed the use of real time qRT-PCR for the detection of free peritoneal tumor cells from patients affected with gastric cancer: a greater sensitivity of real time qRT-PCR was reported in comparison with cytology: all patients who presented peritoneal carcinomatosis during the follow up period were positive at time of surgery for real time qRT-PCR on peritoneal washes and omentum while only about 30% of them were positive even for conventional cytology.

After 1998 some more Authors, mostly Japanese, reported about the use of real time qRT-PCR for the detection of isolated peritoneal tumor cells from gastric cancer patients and all of them concluded confirming how real time qRT-PCR is a more specific and sensitive technique than cytopathology and that it was found to be as independent prognostic marker. Similar studies about colorectal cancer are also present in the literature, but less frequently. In their study Guller et al. (Guller et al., 2002) report that, on a total of 39 colorectal cancer patients, 10 of them resulted positive for the RT-PCR (CEA and CK20) at the peritoneal lavage. During the

follow up period 8 of them had recurrence and positive peritoneal real time qRT-PCR was found to be an independent prognostic factor.

Hara et al. (Hara et al., 2007) published the first and only study comparing the results of RT-PCR on peritoneal lavage in gastric and colorectal cancer patients. They found that prognosis in positive RT-PCR patients was worse in both colorectal and gastric cancer; they also found that, among real time qRT-PCR positive cases, peritoneal carcinomatosis was significantly more frequent in gastric cancer patients but not in colorectal patients. They concluded stating that colorectal carcinoma cells must have some biological characteristics that make them with a low-peritoneal metastatic potential.

Some criticism have been moved to this molecular technique, since some Authors believe that the expression of some genes used for the identification of tumor cells may be present in inflammatory cells as well, resulting real time qRT-PCR in a high sensitivity and low specificity test (Kowalewska et al., 2008).

Some problems about the optimization of the molecular techniques still have to be debated: for example, the possibility of high rate of false positive diagnosis at RT-PCR. This can be due to an illegitimate expression of marker genes in noncancerous cells (Goeminne et al., 1999) or to a too high sensitivity of the technique that can even detect mRNA markers from a very small, clinically insignificant, number of cells. Nevertheless in some Japanese Institutions real time qRT-PCR is already used in the clinical practice: patients with negative cytology and positive real time qRT-

PCR at preoperative staging laparoscopy are treated with a short-term intraperitoneal chemotherapy (Mori et al., 2004).

To our knowledge nothing is reported about the use of IF for the detection of free peritoneal cancer cells in enriched samples of peritoneal lavages. Our study combined for the first time the use of real time qRT-PCR with IF and immunomagnetic enrichment of epithelial cells to detect free peritoneal tumor cells in gastric and colorectal cancer. For each technique we used two different markers: CEA and CK20 for the qRT-PCR and CEA and EpCAM for IF. Our results confirmed the low sensitivity of the traditional cytology: in fact, it was positive only in four cases of gastric cancer with associated massive peritoneal carcinomatosis and in none of colorectal cancers. All cytological positive samples resulted positive also for IF and real time qRT-PCR. On the contrary, no false positive were found at the qRT-PCR or IF examination in the group of patients with non-malignant diseases, further demonstrating the validity of our procedure.

In comparison with cytology, both IF and real time qRT-PCR showed higher positivity rates, being 15% and 78% for gastric cancer patients and 17% and 42% for colorectal cancer patients respectively. Among the gastric cancer patients, IF was positive not only in the 3 of them with massive carcinomatosis, but also in 1 case with minor extent of peritoneal dissemination. Interestingly, in colorectal cancer patients we found positivity even in early stages of disease.

The positivity rate for qRT-PCR in gastric cancer patients was impressive, comprising more than 3/4 of the patients, distributed in all T1-T4 stages of disease.

In contrast, in colorectal cancer patients the qRT-PCR positivity was found in less than half of patients, most of them with T3-T4 disease. All patients positive at IF were also positive at qRT-PCR, except for one colon cancer and one gastric cancer patients.

Our data showed how positive IF resulted to be significantly associated to grading, depth of invasion, stage of disease and cytology in gastric cancer. On the opposite for colorectal cancer IF was note related to any of the examined clinicopathological factors. In the survival study positive IF was associated to worse overall and disease free survival in gastric patients at the univariate analysis; at the multivariate analysis IF was not found to be an independent prognostic factor in gastric cancer patients. In colorectal cancer cases IF was not a statistically significant prognostic factor in both univariate and multivariate analysis.

RT-PCR positivity was associated to higher grading in gastric cancer and only to positive IF in colorectal cancer. In both gastric and colorectal cancer RT-PCR was found to be one of the strongest independent prognostic factors.

From these data we can notice that IF seems to be associated to the most common clinicopathological factors in GC, but it has no prognostic value in both gastric and colorectal cancer patients. On the other hand RT-PCR is not frequently associated to other clinicopathological factors but resulted to be independently relevant for the prognosis in both gastric and colorectal cancer.

In conclusion, we believe that the combination of conventional real time qRT-PCR with immunoenrichment and IF, which permit morphological assessment and

unequivocal identification of the FPTCs as well as validation of the molecular analysis, could be an useful and more powerful procedure for the detection of free peritoneal tumor cells. More studies on these cells are requested to understand their prognostic power and any other possible clinical application. Since the treatment of cancer is going toward the personalized therapy, as well as for the circulating tumor cells, in the future the characterization of peritoneal tumor cells may be interrogated to guide molecularly targeted therapies, assess treatment effect and detect development of drug resistance.

4. References.

- Alkhamesi NA, Ziprin P, Pfistermuller K, Peck DH, Darzi AW. (2005) ICAM-1 mediated peritoneal carcinomatosis, a target for therapeutic intervention. *Clin Exp Metastasis* 22:449-459.
- Baba H, Korenaga D, Okamura T., Saito A and Sugimachi K. (1989) Prognostic factors in gastric cancer with serosal invasion. *Arch Surg* 124:1061-1064.
- Bando E, Yonemura Y, Takeshita Y, et al. (1999) Intraoperative lavage for cytological examination in 1297 patients with gastric carcinoma. *Am J Surg* 178:256-262.
- Benevolo M, Mottolese M, Cosimelli M, et al. (1998) Diagnostic and prognostic value of peritoneal immunocytology in gastric cancer. *J Clin Oncol* 16:3406-3411.
- Benevolo M, Mottolese M, Cosimelli M, Tedesco M, Giannarelli D, Vasselli S, et al. (1998) Diagnostic and prognostic value of peritoneal immunocytology in gastric cancer. *J Clin Oncol* 16:3406-11.
- Bouvy ND, Marquet RL, Jeekel J, Bonjer HJ. (1997) Laparoscopic surgery is associated with less tumour growth stimulation than conventional surgery: An experimental study. *Br J Surg* 84: 358–61.

- Cabourne EJ, Roberts G, Goldin R, Ryder T, Mobberly M, Ziprin P. (2010) Investigation of tumor-peritoneal interactions in the pathogenesis of peritoneal metastases using a novel ex vivo peritoneal model. *J Surg Res* 164:e265-272.
- Cannistrà SA, Kansas GS, Niloff J, DeFranzo B, Kim Y, Ottensmeier C. (1993). Binding of ovarian cancer cells to peritoneal mesothelium in vitro is partly mediated by CD44h. *Cancer Res* 53: 3830–8.
- Casey RC, Koch KA, Oegema TR Jr, Skubitz KM, Pambuccian SE, Grindle SM, Skubitz AP. (2003) Establishment of an in vitro assay to measure the invasion of ovarian carcinoma cells through mesothelial cell monolayers. *Clin Exp Metastasis* 20:343-356.
- Ceelen WP, Bracke ME. (2009) Peritoneal minimal residual disease in colorectal cancer: mechanisms, prevention, and treatment. *Lancet Oncol* 10:72-79.
- Gervasoni A, Monasterio Munoz RM, Wengler GS, Rizzi A, Zaniboni A, Parolini O. (2008) Molecular signature detection of circulating tumor cells using a panel of selected genes. *Cancer letters* 263:267-279.
- Goeminne JC, Guillaume T, Salmon M, Machiels JP, D'Hondt V, Symann M. (1999) Unreliability of carcinoembryonic antigen (CEA) reverse transcriptase-polymerase chain reaction (RT-PCR) in detecting

contaminating breast cancer cells in peripheral blood stem cells due to induction of CEA by growth factors. *Bone Marrow Transplant* 24:769-75.

- Guller U, Zajac P, Schnider A, et al. (2002) Disseminated single tumor cells as detected by real-time quantitative polymerase chain reaction represent a prognostic factor in patients undergoing surgery for colorectal cancer. *Ann Surg* 236:768-75.
- Hagiwara A, Takahashi T, Kojima O, et al. (1992) Prophylaxis with carbon adsorbed mitomycin against peritoneal recurrence of gastric cancer. *Lancet* 339:629-631.
- Hara M, Nakanishi H, Jun Q, et al. (2007) Comparative analysis of intraperitoneal minimal free cancer cells between colorectal and gastric cancer patients using quantitative RT-PCR: possible reason for rare peritoneal recurrence in colorectal cancer. *Clin Exp Metastasis* 24:179-89.
- Harada N, Mizoi T, Kinouchi M, Hoshi K, Ishii S, Shiiba K, Sasaki I, Matsuno S. (2001) Introduction of antisense CD44S CDNA down-regulates expression of overall CD44 isoforms and inhibits tumor growth and metastasis in highly metastatic colon carcinoma cells. *Int J Cancer* 91:67-75.
- Hayashi K, Jiang P, Yamauchi K, et al. (2007). Real-time imaging of tumor cell shedding and trafficking in lymphatic channels. *Cancer Res* 67: 8223–28

- Hayes N, Wayman J, Wadehra V, Schott DJ, Raimes SA, Griffin SM. (1999) Peritoneal cytology in the surgical evaluation of gastric carcinoma. *Br. J Cancer* 79:520-4
- Heyman L, Kellouche S, Fernandes J, Dutoit S, Poulain L, Carreiras F. (2008) Vitronectin and its receptors partly mediate adhesion of ovarian cancer cells to peritoneal mesothelium in vitro. *Tumour Biol* 29:231-244.
- Hofer SO, Shrayer D, Reichner JS, Hoekstra HJ, Wanebo HJ. (1998) Wound-induced tumor progression: A probable role in recurrence after tumor resection. *Arch. Surg.* 133: 383–9
- Ivarsson ML, Holmdahl L, Falk P, Mölne J, Risberg B. (1998) Characterization and fibrinolytic properties of mesothelial cells isolated from peritoneal lavage. *Scand J Clin Lab Invest* 58:195-203.
- Jayne DG, Fook S, Loi C, Seow-Choen F. (2002) Peritoneal carcinomatosis from colorectal cancer. *Br J Surg* 89:1545-1550.
- Jayne DG, O'Leary R, Gill A, Hick A, Guillou PJ. (1999) A three-dimensional in-vitro model for the study of peritoneal tumour metastasis. *Clin Exp Metastasis* 17:515-523.
- Jones LM, Gardner MJ, Catterall JB, Turner GA. (1995) Hyaluronic acid secreted by mesothelial cells: A natural barrier to ovarian cancer cell adhesion. *Clin. Exp. Metastasis* 13: 373–80.

- Juhl H, Stritzel M, Wroblewski A, Henne-Bruns D, et al. (1994) Immunocytological detection of micrometastatic cells: comparative evaluation of findings in the peritoneal cavity and the bone marrow of gastric, colorectal and pancreatic cancer patients. *Int J Cancer* 57:330-335.
- Kajiyama H, Shibata K, Terauchi M, Ino K, Nawa A, Kikkawa F. (2008) Involvement of SDF-1α / CXCR4 axis in the enhanced peritoneal metastasis of epithelial ovarian carcinoma. *Int J Cancer* 122:91-99.
- Katsuragi K, Yashiro M, Sawada T, Osaka H, Ohira M, Hirakawa K. (2007) Prognostic impact of PCR-based identification of isolated tumour cells in the peritoneal lavage fluid of gastric cancer patients who underwent a curative R0 resection. *Br J Cancer* 97:550-6.
- Khair G., Monson. J.R., Greenman J. (2007) Epithelial molecular markers in the peripheral blood of patients with colorectal cancer. *Dis. Colon Rectum* 50:1188-1203.
- Kodera Y, Nakanishi H, Ito S, et al. (2002) Quantitative detection of disseminated free cancer cells in peritoneal washes with real-time reverse transcriptase-polymerase chain reaction: a sensitive predictor of outcome for patients with gastric carcinoma. *Ann Surg* 235: 99-506.
- Kodera Y, Nakanishi H, Yamamura Y, et al. (1998) Prognostic value and clinical implications of disseminated cancer cells in the peritoneal cavity

detected by reverse transcriptase-polymerase chain reaction and cytology. *Int J Cancer* 79:429-33.

- Kodera Y, Yamamura Y, Shimizu Y, et al. (1999) Peritoneal washing cytology: prognostic value of positive findings in patients with gastric carcinoma undergoing a potentially curative resection. *J Surg Oncol* 72:60-64.
- Kovacs D, Raffa S, Flori E, Aspite N, Briganti S, Cardinali G, Torrisi MR, Picardo M. (2009) Keratinocyte growth factor down-regulates intracellular ROS production induced by UVB. *J Dermatol Sci* 54:106-113.
- Kowalewska M, Chechlinska M, Nowak R. (2008) Carcinoembryonic antigen and cytokeratin 20 in peritoneal cells of cancer patients: are we aware of what we are detecting by mRNA examination? *Br J Cancer* 98:512-3.
- Ksiazek K, Mikuła-Pietrasik J, Catar R, Dworacki G, Winckiewicz M, Frydrychowicz M, Dragun D, Staniszewski R, Jörres A, Witowski J. (2010) Oxidative stress-dependent increase in ICAM-1 expression promotes adhesion of colorectal and pancreatic cancers to the senescent peritoneal mesothelium. *Int J Cancer* 127:293-303.
- Ksiazek K, Mikuła-Pietrasik J, Jörres A, Witowski J. (2008) Oxidative stress-mediated early senescence contributes to the short replicative life span of human peritoneal mesothelial cells. *Free Radic Biol Med* 45:460-467.
- Ksiazek K, Mikula-Pietrasik J, Korybalska K, Dworacki G, Jörres A, Witowski J. (2009) Senescent peritoneal mesothelial cells promote ovarian

cancer cell adhesion: the role of oxidative stress-induced fibronectin. *Am J Pathol* 174:1230-1240.

- La Torre M, Ferri M, Giovagnoli MR, Sforza N, Cosenza G, Giarnieri E, Ziparo V. (2010) Peritoneal wash cytology in gastric carcinoma. Prognostic significance and therapeutic consequences. *Eur J Surg Oncol* 36:982-6.
- Moertel CG, Rleming TR, MacDonald JS, et al. (1990) Levamisole and fluorouracil for adjuvant therapy of resected colon carcinoma. *N Engl J Med* 322:352-358.
- Mori T, Fujiwara Y, Sugita Y, et al. (2004) Application of molecular diagnosis for detection of peritoneal micrometastasis and evaluation of preoperative chemotherapy in advanced gastric carcinoma. *Ann Surg Oncol* 11:14-20.
- Nekarda H, Gess C, Stark M, Mueller JD, Fink U, Schenck U, Siewert JR. (1999) Immunocytochemically detected free peritoneal tumour cells (FPTC) are a strong prognostic factor in gastric carcinoma. *Br J Cancer* 79:611-619.
- Noura S, Ohue M, Seki Y, Yano M, Ishikawa O, Kameyama M. (2009) Long-term prognostic value of conventional peritoneal lavage cytology in patients undergoing curative colorectal cancer resection. *Dis Colon Rectum* 52:1312-20.
- Oyama K, Terashima M, Takagane A, Maesawa C. (2004) Prognostic significance of peritoneal minimal residual disease in gastric cancer detected by reverse transcription-polymerase chain reaction. *Br J Surg* 19:435-43.

- Pantel K, Brakenhoff RH, Brandt B. (2008) Detection, clinical relevance and specific biological properties of disseminating tumour cells. *Nat Rev Cancer* 8:329-40.
- Sadeghi B, Arvieux C, Glehen O et al. (2000) Peritoneal carcinomatosis from nongynecologic malignancies: results of the EVOCAPE 1 multicentric prospective study. *Cancer* 88:358-363.
- Saito Y, Sekine W, Sano R, Komatsu S, Mizuno H, Katabami K, Shimada K, Oku T, Tsuji T. (2010) Potentiation of cell invasion and matrix metalloproteinase production by $\alpha 3\beta 1$ integrin-mediated adhesion of gastric carcinoma cells to laminin-5. *Clin Exp Metastasis* 27:197-205.
- Sakakura C, Takemura M, Hagiwara A, et al. (2004) Overexpression of dopa decarboxylase in peritoneal dissemination of gastric cancer and its potential as a novel marker for the detection of peritoneal micrometastases with real-time RTPCR. *Br J Cancer* 90:665-671.
- Schott A, Vogel I, Krueger U, et al. (1998) Isolated tumor cells are frequently detectable in the peritoneal cavity of gastric and colorectal cancer patients and serve as a new prognostic marker. *Ann. Surg* 227:372-9.
- Sikkink CJ, Reijnen MM, Duffhues BA, de Man BM, Lomme RM, van Goor H. (2009) Intercellular adhesion molecule-1 and gelatinase expression in human peritoneal mesothelial cells during propagation in culture. *Transl Res* 153:240-248.

- Sugarbaker PH, Yonemura Y (2000) Clinical pathway for the management of resectable gastric cancer with peritoneal seeding: best palliation with a ray of hope for cure. *Oncology* 58:96-107.
- Takatsuki H, Komatsu S, Sano R, Takada Y, Tsuji T. (2004) Adhesion of gastric carcinoma cells to peritoneum mediated by $\alpha 3\beta 1$ integrin (VLA-3). *Cancer Res* 64:6065-6070.
- Torrisi MR. (2004) Differential response to keratinocyte growth factor receptor and epidermal growth factor receptor ligands of proliferating and differentiating intestinal epithelial cells. *J Cell Physiol* 200:31-44.
- van den Tol PM, van Rossen EE, van Eijck CH, Bonthuis F, Marquet RL, Jeekel H. (1998). Reduction of peritoneal trauma by using nonsurgical gauze leads to less implantation metastasis of spilled tumor cells. *Ann Surg* 227: 242–8.
- van Grevenstein WM, Hofland LJ, van Rossen ME, van Koetsveld PM, Jeekel J, van Eijck CH. (2007) Inflammatory cytokines stimulate the adhesion of colon carcinoma cells to mesothelial monolayers. *Dig Dis Sci* 52:2775-2783.
- Visco V, Belleudi F, Marchese C, Leone L, Aimati L, Cardinali G, Kovacs D, Frati L,
- Wind P, Norklinger B, Roger V, Kahlil A, Guin E, Parc R. (1999) Long-term prognostic value of positive peritoneal washing in colon cancer. *Scand J Gastroenterol* 34:606-10.

- Wu CC, Chen JT, Chang MC, et al. (1997) Optimal surgical strategy for potentially curable serosainvolved gastric carcinoma with intraperitoneal free cancer cells. *J Am Coll Surg* 184: 611-617.
- Yung S, Li FK, Chan TM. (2006) Peritoneal mesothelial cell culture and biology. *Perit Dial Int* 26:162-173.
- Ziprin P, Ridgway PF, Pfistermüller KL, Peck DH, Darzi AW. (2003) ICAM-1 mediated tumor-mesothelial cell adhesion is modulated by IL-6 and TNF-alpha: a potential mechanism by which surgical trauma increases peritoneal metastases. *Cell Commun Adhes* 10:141-154.

Index